

CCL17 signals through CCR8 to induce CCL3 expression and restrain atheroprotective Tregs

Yvonne Döring^{#,*1,2,3}, Emiel P.C. van der Vorst^{#1,3,4,5,6}, Yi Yan^{#1,3}, Carlos Neideck^{#1}, Xavier Blanchet¹, Yvonne Jansen¹, Manuela Kemmerich¹, Soyolmaa Bayasgalan¹, Linsey J.F. Peters^{1,4,5,6}, Michael Hristov¹, Changjun Yin^{1,3,8}, Xi Zhang¹, Julian Leberzammer^{1,3}, Inhye Park⁹, Selin Gencer¹, Andreas Habenicht^{1,3}, Alexander Fausner¹, Daniel Teupser¹⁰, Claudia Monaco⁹, Lesca Holdt¹⁰, Philipp von Hundelshausen¹, Christian Weber^{*,1,3,7,8}

¹Institute for Cardiovascular Prevention (IPEK), LMU Munich, Munich, Germany;

²Division of Angiology, Swiss Cardiovascular Center, Inselspital, Bern University Hospital, University of Bern, Switzerland;

³DZHK (German Centre for Cardiovascular Research), partner site Munich Heart Alliance, Munich, Germany;

⁴Interdisciplinary Center for Clinical Research (IZKF), RWTH Aachen University, Aachen, Germany;

⁵Institute for Molecular Cardiovascular Research (IMCAR), RWTH Aachen University, Aachen, Germany;

⁶Department of Pathology, Cardiovascular Research Institute Maastricht (CARIM), Maastricht University Medical Centre, Maastricht, the Netherlands;

⁷Department of Biochemistry, Cardiovascular Research Institute Maastricht (CARIM), Maastricht University, the Netherlands;

⁸Munich Cluster for Systems Neurology (SyNergy), Munich, Germany;

⁹The Kennedy Institute of Rheumatology, Nuffield Department of Orthopedics, Rheumatology and Musculoskeletal Sciences, University of Oxford, United Kingdom;

¹⁰Institute of Laboratory Medicine, University Hospital, LMU Munich, Germany.

#These authors contributed equally to the manuscript and share authorship.

**Correspondence to:*

Yvonne Döring or Christian Weber

Institute for Cardiovascular Prevention, Ludwig-Maximilians-University Munich

Pettenkoflerstraße 8a und 9, D-80336 München, Germany

Tel.: +49 89 4400 54610; Fax: +49 89 4400 54352

Email: ydoering@med.lmu.de or chweber@med.lmu.de

Keywords:

chemokines, chemokine receptors, atherosclerosis, regulatory T cells

Abstract

The CC chemokine CCL17 plays diverse and seemingly opposing roles in immune homeostasis. CCL17 signals through CCR4 on regulatory T cells (Tregs) to promote their tissue localization. Also, CCL17 is produced by a subset of conventional dendritic cells (cDCs) and drives chronic inflammation and atherosclerosis by suppressing Treg functions through yet undefined mechanisms. We found that cDCs from CCL17-deficient mice displayed a pro-tolerogenic phenotype and transcriptomic profile that, surprisingly, was not phenocopied in mice lacking CCR4, thus indicating the involvement of an alternative pathway. We identified CCL3 as the only cytokine/chemokine decreased in plasma of CCL17-deficient mice. Correspondingly, CCL3 expression in cDCs and T cells was induced by CCL17 in the absence of CCR4. We provide several lines of evidence that CCR8 serves as a functional high-affinity CCL17 receptor expressed in CD4⁺ Tregs and that CCL17 signaling through CCR8 induces CCL3 expression in Tregs and suppresses their functions. Genetic deficiencies of CCL3, and of CCR8 in CD4⁺ T cells, as well as blockade of CCR8, reduced CCL3 secretion, boosted FoxP3⁺ Treg numbers and limited atherosclerosis. Conversely, the administration of CCL3 exacerbated atherosclerosis and restrained Treg differentiation. In symptomatic versus asymptomatic human carotid atheroma, CCL3 expression was increased, while FoxP3 expression was reduced. Collectively, our data establish a novel chemokine pathway whereby CCL17 interacts with CCR8 to yield a CCL3-dependent suppression of atheroprotective Tregs.

Introduction

Atherosclerosis is a lipid-driven chronic inflammatory disease of the arterial wall, underlying the majority of cardiovascular diseases (CVD).¹ Among other immune cells, dendritic cells (DCs) have been identified in healthy and inflamed arterial intima of mice and men²⁻⁴, and advanced human plaques contain an increased number of DCs in clusters with T cells.⁵ The chemokine CCL17 (previously known as thymus and activation-regulated chemokine, TARC) was shown to be elevated in patients with CVD⁶ and atopic dermatitis, who are also more prone to develop CVD.^{7,8} Furthermore, an intronic single nucleotide polymorphism at rs223828 corresponds with increased CCL17 serum levels and increased CVD risk in humans⁹, and mouse studies have revealed a pro-inflammatory role of CCL17 in atherosclerosis¹⁰ and colitis¹¹. CCL17 is primarily expressed by a subset of conventional dendritic cells (cDCs), antigen-presenting cells, which express MHC class II and migrate to draining lymph nodes (LNs) to prime naive T cells, and plays a crucial role in the recruitment and migration of various T-cell subsets, including a subpopulation of CD4⁺ T cells, regulatory T cells (Tregs)^{12,13-15}. Tregs use multiple effector mechanisms to modulate immune system responses and to ensure the balance between immune activation and tolerance towards self-antigens¹⁶. Naturally arising CD4⁺CD25⁺ Tregs have been shown to control the development of atherosclerosis and have also been implicated in the regression of established atherosclerotic lesions by licensing pro-resolving macrophage functions.^{17,18} Our previous work has revealed that CCL17 controls Treg homeostasis, restraining their expansion and thereby promoting atherosclerosis.¹⁰ Accordingly, the genetic deficiency of CCL17 decreased atherosclerotic plaque burden by facilitating Treg expansion and survival, and blocking CCL17 with a monoclonal antibody resulted in Treg expansion in lymphoid organs and reduced atheroprotection.¹⁰ However, the precise mechanisms by which DC-derived CCL17 controls Treg homeostasis remain to be elucidated, in particular those involving relevant soluble mediators or receptors.

Of note, CCR4 is the only cognate signaling receptor for CCL17 identified and confirmed to date, well-known to contribute to the recruitment and in vivo function of Tregs.¹⁹ Yet, CCR4 deficiency did not phenocopy the effects on Tregs and protection from atherosclerosis observed in CCL17-deficient mice.¹⁰ Analogous findings were obtained in a model of atopic dermatitis, where the inflammatory burden was reduced in mice lacking CCL17 but not CCR4.²⁰ Consistently, deficiency in DC-derived CCL17 was protective against intestinal inflammation in a mouse model of colitis by creating a cytokine milieu that facilitated Treg expansion and, likewise, did not require CCR4.¹¹ In conjunction, these results suggest the existence of an alternative CCR4-independent receptor pathway triggered by CCL17. Here, we provide, to our knowledge, the first unequivocal evidence that CCL17 signals via CCR8 its alternative high-affinity receptor expressed on T-cell and DC subsets, harnessing their release

of CCL3 as an autocrine and paracrine mediator and thus leading to the suppression of atheroprotective Tregs.

Results

CCR4 does not mediate effects of CCL17 on atherogenesis

In line with previous results¹⁰, mice with a targeted replacement of the *Ccl17* gene by the *enhanced green fluorescent protein* gene (*eGFP*; *Apoe*^{-/-}*Ccl17*^{e/e} mice) displayed a significant reduction of atherosclerotic lesions in the aortic root, thoraco-abdominal aorta and aortic arch after 12 weeks of western-type diet (WD) as compared to *Apoe*^{-/-} littermate controls (**Supplemental Figure 1a-d**). This was accompanied by a higher frequency of CD25⁺Foxp3⁺CD3⁺CD4⁺ regulatory T cells (Treg) in para-aortic LNs and spleens (**Supplemental Figure 1e,f**, see **Supplemental Figure 1g** for gating strategy) and in axillary and inguinal LNs of *Apoe*^{-/-}*Ccl17*^{e/e} mice as compared to controls (**Supplemental Figure 1h-j**). In contrast, mice lacking the canonical CCL17 receptor CCR4 did not phenocopy the modifications observed in CCL17-deficient mice. Neither hematopoietic CCR4 deficiency¹⁰ nor somatic deletion in *Apoe*^{-/-}*Ccr4*^{-/-} mice altered atherosclerotic lesion size or Treg frequencies compared to *Apoe*^{-/-} controls after 12 weeks of WD (**Figure 1a-1f** and **Supplemental Figure 1k-n**). Also, a decrease in apoptotic Treg reported in LNs of CCL17-deficient mice¹⁰ was not found in LN of CCR4-deficient mice (**Supplemental Figure 1o**). Cholesterol and triglyceride plasma levels, as well as circulating leukocyte and thrombocyte counts did not differ between *Apoe*^{-/-}*Ccl17*^{e/e}, *Apoe*^{-/-}*Ccr4*^{-/-} and respective control mice (**Supplemental Table 1 and 2**) suggesting that the observed phenotype was not secondary to changes in lipid metabolism or disbalances in blood. Using recombinant CCL17, CCL22 and the CCR4 inhibitor C021 in Transwell assays, we confirmed CCR4-dependent chemotaxis of CD4⁺ T cells isolated from *Apoe*^{-/-} mice and from human PBMCs *in vitro* (**Supplemental Figure 2a,b**). Notably, C021 abrogated CCL22-induced migration to a greater extent than CCL17-induced migration (**Supplemental Figure 2a,b**). Also, blocking CCR8 by a specific antibody significantly reduced CCL17-induced chemotaxis of human CD4⁺ T cells to comparably to blocking CCL1-induced migration (**Supplemental Figure 2c**). Taken together, these data indicate that an alternative signaling pathway might be involved in mediating the effects of CCL17. In the context of Treg homeostasis, this notion was reinforced also by the subsequent experiments. Co-culturing CD4⁺CD62L⁺ T cells with *ex vivo* isolated cDCs revealed an increased differentiation of CD4⁺CD25⁺Foxp3⁺ Tregs in the presence of *Apoe*^{-/-}*Ccl17*^{e/e} cDCs but not *Apoe*^{-/-}*Ccr4*^{-/-} or *Apoe*^{-/-} cDCs (**Figure 1g**). To establish whether CCL17-deficient cDCs differentially express putative mediators responsible for this effect, we FACS-sorted CD45⁺CD11c⁺CD3⁻CD19⁻ cells from LNs of *Apoe*^{-/-}*Ccl17*^{wt/e} or *Apoe*^{-/-}*Ccl17*^{e/e} mice and performed single-cell RNA sequencing (scRNAseq). Our analysis identified seven different DC clusters (**Figure 1h** and **Supplemental Figure 3**), with CCL17-expressing eGFP⁺ cells almost exclusively located within CCR7⁺ cDC clusters (**Supplemental Figure 3a-c**). In CCL17-deficient samples, CCR7⁺ cDCs were enriched in number and CCR7⁺ cDCs in general had a higher tolerogenic score

compared to other DC clusters (**Figure 1i**). A tolerogenic profile was defined by high expression of *Aldh1a2*, *CD83* and *CD273* in CCR7⁺ cDCs (**Figure 1i and Supplemental Figure 3d-g**) and analysis of a set of genes (**Supplemental Table 3**) defining immunogenic and tolerogenic cell properties (see Methods for details). Although the tolerogenic score did not differ between hetero- and homozygous samples, the number of tolerogenic cDCs was significantly higher in CCL17-deficient mice (**Figure 1j**), indicating that more cDCs acquire a tolerogenic phenotype in the absence of CCL17. In support of our RNAseq analysis, flow cytometry of cDCs in aortic LNs of *Apoe*^{-/-} and *Apoe*^{-/-}*Ccl17*^{+/e} mice uncovered a significantly higher percentage of CD83⁺ and CCR7⁺ DCs among cDCs (**Supplemental Figure 3h,i**). Deletion of CD83 in cDCs has been found to confer a pro-inflammatory DC phenotype fostering antigen-dependent T-cell proliferation and Th17 commitment, whereas Treg suppressive capacity is subverted hindering inflammation-resolving mechanisms.²¹ In addition, Gene Set Variation Analysis (GSVA) revealed an enrichment of pro-inflammatory pathways in CCL17-competent cDCs (**Supplemental Figure 3 j-l**). These data are in line with an atheroprotective role for CCR7 as observed using an *Apoe*^{-/-} mouse model.^{22,23}

CCL17 induces CCL3 release independent of CCR4 expression

Because CCL17-deficient mice displayed increased numbers of tolerogenic cDCs, we performed an unbiased screening for inflammatory mediators differentially regulated in these mice. Using a multiplex-bead-array to measure concentrations of cytokines and chemokines, we identified only CCL3 to be significantly reduced in plasma of *Apoe*^{-/-}*Ccl17*^{+/e} mice after 12 weeks of WD as compared to their *Apoe*^{-/-} controls (**Figure 2a,b; Supplemental Table 4**). This also corresponded with the decreased lesion size and increased Treg numbers in *Apoe*^{-/-}*Ccl17*^{+/e} mice (**Supplemental Figure 1**). In contrast, CCL3 plasma levels in *Apoe*^{-/-}*Ccr4*^{-/-} mice were unaffected (**Figure 2a,c**), consistent with their unaltered atherosclerotic burden (**Figure 1a-f**). Reconstituting *Apoe*^{-/-}*Ccl17*^{+/e} mice with CCL17-sufficient bone marrow restored CCL3 plasma levels to those seen in *Apoe*^{-/-} control mice (**Figure 2d,e**). Given that CCL3 titers were diminished in systemic circulation of CCL17-deficient mice, we next evaluated which cell types release CCL3 in response to CCL17. To this end, we sorted CD11c⁺MHCII⁺ cDCs, CD3⁺ T cells and CD19⁺B220⁺ B cells from LNs and isolated monocytes and neutrophils from spleen and bone marrow and treated them with CCL17 *in vitro*. ELISA identified cDCs and T cells as the main source of CCL3 after CCL17 stimulation, whereas CCL3 release was low or negligible from monocytes, B cells and neutrophils (**Figure 2f**). CCL3 release was induced by CCL17 in different T cell subsets, including splenic CD4⁺ T helper cells, CD4⁺CD62L⁺ naïve T cells/memory T cells and CD4⁺CD25⁺ Tregs (**Figure 2g**). Comparing FACS-sorted CCL17⁺ (eGFP⁻) with CCL17-deficient CD11c⁺MHCII⁺ cDCs (eGFP⁺), we found that baseline CCL3 secretion was significantly lower in CCL17-deficient cDCs, whereas CCL17-stimulated CCL3

release was comparable (**Figure 1h**), suggesting that CCL17 released by CCL17⁺ cDCs can act in an autocrine or a paracrine fashion to induce CCL3 secretion. Treatment with the CCR4 inhibitor C021 revealed that upregulation of CCL3 release by CCL17 was independent of CCR4 in cDCs (**Figure 2i**) and CD4⁺ T cells (**Figure 2j**), indicating that CCL17 mediates CCL3 secretion through a putative alternative receptor.

CCL17 binds and activates CCR8 as a non-canonical receptor

In search for an alternative CCL17 receptor that might mediate the release of CCL3 from DCs, we revisited the notion that CCR8 could be a receptor for CCL17²⁴ (findings subsequently contested²⁵) especially as CCR8 has also been implicated in controlling the migration and function of Tregs.^{26,27} To probe for binding of CCL17 to CCR8, we used surface plasmon resonance (SPR) to record the concentration-dependent binding of CCR8-carrying liposomes to biotinylated CCL17 immobilized on a BIAcore C1 sensor chip, with CCR4-carrying, mock protein-carrying and pure liposomes serving as positive or negative controls, respectively (**Figure 3a-c**). CCR8-bearing liposomes displayed saturable binding with a K_D (k_{off}/k_{on}) calculated to be 1.1 ± 0.4 nM, indicating a high-affinity interaction between CCL17 and CCR8 (**Figure 3b,c**). While CCR4-bearing liposomes showed even stronger binding, irrelevant protein-bearing or empty liposomes did not support binding on CCL17 (**Figure 3a**). A CCL5-chip did not support any binding (data not shown). To confirm these findings, we used a proximity ligation assay in CCR4- or CCR8-transfected Jurkat cells or in adherent cDCs from LNs of *Apoe*^{-/-} mice treated with CCL17 or the cognate CCR8 ligand CCL1 and subsequently with non-blocking antibodies to CCL17 or CCL1 and to CCR4, CCR8, or CCR5 (DCs only) to yield ligation signals detecting receptor interactions of CCL17 and CCL1. Proximity ligation signals and their quantification revealed an interaction of CCL17 with both CCR4 and CCR8, whereas CCL1 interacted with CCR8 but not with CCR4 (**Figure 3d,e, Supplemental Fig. 2d,e**). Moreover, we performed receptor binding competition studies in human CCR8-expressing HEK293 transfectants using fluorescently labeled CCL1 and CCL17. Inhibition of CCL1^{AF647} binding to CCR8-transfectants with increasing concentrations of unlabeled CCL17 yielded an IC_{50} 9.4 nM, whereas inhibition of CCL17^{AF647} binding to CCR8-transfectants with increasing concentrations of unlabeled CCL1 yielded an IC_{50} 0.58 nM (**Figure 3f,g**). Using primary CD4⁺ T cells isolated from thymus or LNs of tamoxifen-inducible CCR8-competent *Uni*^{CreErt2-} *Ccr8*^{flox/flox} (*CCR8*^{WT} *Apoe*^{-/-}) or CCR8-deficient *Uni*^{CreErt2+} *Ccr8*^{flox/flox} (*CCR8*^{KO} *Apoe*^{-/-}) *Apoe*^{-/-} mice, we found CCR8 internalization upon CCL17 treatment in CCR8-expressing cells but not in CCR8-deficient T cells (**Figure 3h,i**). In addition, human CD4⁺ T cells exhibited both CCR4 and CCR8 internalization upon CCL17 treatment, whereas CCL1 induced only that of CCR8 and CCL22 induced only that of CCR4 (**Figure 3j,k**). These experiments clearly indicate that CCL17 binds to CCR8.

To test whether CCL17 can elicit Gi signaling via CCR8, we determined downstream cAMP levels in Glosensor-HEK293 cells transfected with CCR4 or CCR8 and stimulated with recombinant human CCL17, CCL1 or CCL20 (**Figure 4a,b**). Previous studies reported CCL17 binding to CCR8 but lack of subsequent calcium signaling.²⁴ In contrast, our result revealed that CCL17 induced Gi-mediated signaling in both CCR4- and CCR8-transfected cells. CCL1, used as a positive control, induced Gi signaling in CCR8-transfected cells, but not in CCR4-transfected cells, whereas CCL20, as a negative control, did not induce Gi signaling in CCR4 nor CCR8 transfectants (**Figure 4a,b**). Next, we performed Transwell migration assays with CD4⁺ T cells isolated from *CCR8^{WT}Apoe^{-/-}* and *CCR8^{KO}Apoe^{-/-}* mice. The CCL17-induced migration of CD4⁺ T cells lacking CCR8 was markedly reduced, whereas migration towards CCL1 was reduced even more and that towards CCL22 was unaffected (**Figure 4c**). The migration of CD4⁺ T cells induced by CCL17 followed a bell-shaped dose-response curve and was chemotactic in nature, as it was inhibited in a checker-board analysis by CCL17 placed in the upper chamber (**Figure 4d**). Taken together, these data clearly establish that CCL17 binds to CCR8 and that the CCL17-CCR8 interaction induces functional G-protein-coupled signaling and downstream cellular responses.

The CCL17/CCR8-CCL3 axis critically interferes with Treg differentiation

Having established the binding of CCL17 to CCR8, we next assessed which cell types express CCR8. Screening *the Human Protein Atlas* (<https://www.proteinatlas.org>) we found CCR8 to be mostly expressed on T-cell subsets with an enrichment in Tregs (**Supplemental Figure 4a,b**). Accordingly, single cell- RNAseq of aortic LNs from CCL17-competent and CCL17-deficient mice revealed a prominent expression of CCR8 in CD4⁺ T cells, and specifically Tregs and follicular T helper cells featured the highest expression (**Supplemental Figure 4c**). We could also detect CCR8 expression on approximately 15% of cDCs present in LNs (**Supplemental Figure 4d**). Building on our *in vitro* findings that CCL17 binds and signals via CCR8 and induces CCL3 release independently of CCR4, we next assessed directly whether the CCL17-CCR8 pathway mediates CCL3 secretion. To this end, CD4⁺CD62L⁺ T cells sorted from *CCR8^{WT}Apoe^{-/-}* or *CCR8^{KO}Apoe^{-/-}* mice were co-cultured in the absence and presence of CCL17 with CCR8-competent cDCs for 3 days (**Figure 5a**). CCL3 secretion was lower at baseline (i.e. without CCL17) in CCR8-deficient CD4⁺ T cells, and was markedly induced by addition of CCL17 in CCR8-competent but not in CCR8-deficient CD4⁺ T cells (**Figure 5b**). Correspondingly, the number of Tregs in co-cultures of cDCs with CCR8-deficient CD4⁺ T cells was increased, as compared to CCR8-competent controls, and remained higher even upon addition of CCL17 (**Figure 5c**). This indicates that CCL17-induced signaling via CCR8 on CD4⁺ T cells and the subsequent autocrine CCL3 release are of importance in restraining Treg differentiation, whereas cDC-derived paracrine production of CCL3 appears to be rather

redundant.

Next, CD4⁺CD62L⁺ T cells sorted from *CCR8*^{WT}*Apoe*^{-/-} or *CCR8*^{KO}*Apoe*^{-/-} mice were co-cultured with CCL17-competent or CCL17-deficient cDCs for 3 days (**Figure 5d**). Combining CCR8-competent naïve T cells with CCL17-deficient cDCs resulted in reduced CCL3 levels, as compared to CCL17-competent cDCs, while co-cultures with CCR8-deficient naïve T cells showed lower CCL3 levels with either CCL17-competent or CCL17-deficient cDCs (**Figure 5e**). This was accompanied by inverse changes in Treg numbers, which were elevated in the presence of CCL17-deficient cDCs or using CCR8-deficient CD4⁺ T cells independent of CCL17 (**Figure 5f**). To verify the requirement for T cell-derived CCL3, we co-cultured CD4⁺CD62L⁺ T cells from CCL3-competent or CCL3-deficient mice with CCR8-competent cDCs in the absence and presence of CCL17 for 3 days (**Figure 5g**). CCL3 release was markedly induced by CCL17 compared to baseline in CCL3-competent T cells and was abolished in co-cultures with CCL3-deficient CD4⁺ T cells, where the background CCL3 secretion from cDC was less responsive to CCL17 (**Figure 5h**). Correspondingly, the number of Tregs in co-cultures of cDCs with CCL3-deficient CD4⁺ T cells was increased, as compared to controls, and remained higher and not diminished upon addition CCL17 (**Figure 5i**). Together, our data demonstrate that CCL17 interaction with CCR8, particularly on CD4⁺ T cells, is critical in mediating CCL3 secretion and restraining Treg differentiation.

Blockade or CD4⁺ T cell-specific deletion of CCR8 reduce lesion size and increase Tregs

To test whether CCR8 blockade would affect *in vivo* Treg numbers and atherosclerotic lesion size, we injected a blocking antibody to CCR8 or an appropriate isotype control 3-times weekly into *Apoe*^{-/-} mice receiving 4 weeks of WD (**Figure 6a**). The extent of atherosclerotic lesions in aortic roots and arches was significantly reduced in mice treated with CCR8-blocking antibody (**Figure 6b-c**). Accordingly, CCL3 expression was reduced, whereas the number FoxP3⁺CD25⁺ Treg was elevated in para-aortic LNs and spleens of anti-CCR8-treated mice (**Figure 6d-f**). Plasma lipid levels, circulating leukocyte and thrombocyte counts remained unaltered by the anti-CCR8 treatment (**Supplemental Table 5**). Using *CCR8*^{WT}*Apoe*^{-/-} and *CCR8*^{KO}*Apoe*^{-/-} mice fed a WD for 12 weeks, we observed a marked reduction in atherosclerotic lesion size in aortic root and thoraco-abdominal aorta in CCR8-deficient mice (**Supplemental Figure 5a-d**). Because our *in vitro* data indicated a critical importance of CCR8 on CD4⁺ T cells in controlling Treg differentiation, we backcrossed *Ccr8*^{fllox/fllox}*Apoe*^{-/-} mice with *CD4*^{Cre}*Apoe*^{-/-} mice and fed them a WD for 12 weeks (**Figure 6g**). In line with the effects of systemic deletion, we found a significantly reduced atherosclerotic lesion burden in the aortic arch and thoraco-abdominal aorta of mice lacking CCR8 in CD4⁺ T cells (**Figure 6h-i**). Lesional SMC content was increased in mice lacking CD4-specific CCR8 expression but macrophage content was unaltered (**Supplemental Figure 5e-g**). CCL3 expression in LNs of

CD4^{Cre+}Ccr8^{flox/flox}Apoe^{-/-} mice was reduced, whereas Treg numbers in para-aortic LNs and spleens were increased (**Figure 6j-l**). Again, plasma lipid levels, circulating leukocyte and platelet counts did not differ between *CD4^{Cre+}Ccr8^{flox/flox}Apoe^{-/-}* and control mice (**Supplemental Table 6**). This corroborates a crucial role for CCR8 on CD4⁺ T cells in conferring atherogenic effects of CCL17 on CCL3 release, Treg suppression and lesion formation.

CCL3 release induced by CCL17 controls Treg differentiation via CCR1

Having established that CCL17 signaling via CCR8 on CD4⁺ T cells mediates CCL3 release that, in turn, halts Treg differentiation, we next explored which of the cognate receptors (CCR1 or CCR5) for CCL3 is responsible for mediating these effects, both of which are expressed on CD4⁺ T cells (**Supplemental Figure 4e-g**). To this end, we cultured CD4⁺CD62L⁺ T cells isolated from spleens of *Apoe^{-/-}*, *Apoe^{-/-}Ccr1^{-/-}* or *Apoe^{-/-}Ccr5^{-/-}* mice under Treg-polarizing conditions in the presence or absence of CCL3 (**Figure 7a**). Flow cytometry analysis revealed a decrease in CD4⁺CD25⁺Foxp3⁺ Treg frequencies within the CD4⁺ T-cell population, when comparing CCL3-treated cultures from *Apoe^{-/-}* or *Apoe^{-/-}Ccr5^{-/-}* mice to the respective controls (TGFβ only), whereas this did not occur in T cells isolated from *Apoe^{-/-}Ccr1^{-/-}* mice (**Figure 7b**), indicating that CCL3 restrains CD4⁺CD25⁺ Foxp3⁺ Treg differentiation via CCR1. We also evaluated the frequency of CD4⁺FoxP3⁺Tbet⁺ cells as a subset with pro-atherogenic functions²⁸ among CD4⁺ T cells in aortic LNs of our CCL17- and CCL3-deficient mice and could see a clear reduction of these cells in absence of CCL17 or CCL3 (**Supplemental Figure 4h**). We further asked if addition of CCL3 under Treg polarizing conditions might increase the abundance of Th subsets with a more pro-inflammatory profile. FACS analysis revealed an increase in Th₁ (CD4⁺Tbet⁺) and Th₁₇ (CD4⁺Roryt⁺) but no change in Th₂ (CD4⁺Gata3⁺) cell frequencies in CCL3-treated T-cell cultures from *Apoe^{-/-}* or *Apoe^{-/-}Ccr5^{-/-}* mice, as compared to only TGFβ-treated samples (**Supplemental Figure 4i,j and data not shown**). However, Th₁ and Th₁₇ as well as Th₂ frequencies in T cell cultures from *Apoe^{-/-}Ccr1^{-/-}* mice were not altered in absence or presence of rmCCL3, indicating that CCL3 also induces Th₁ and Th₁₇ differentiation (at least partly) in a CCR1-dependent manner also in agreement with its strong pro-inflammatory properties (**Supplemental Figure 4j and data not shown**). To confirm the role of the CCL3-CCR1 axis in the effects of CCL17, we sorted eGFP⁺ cDCs from *Apoe^{-/-}Ccl17^{wt/e}* (CCL17-competent) and *Apoe^{-/-}Ccl17^{e/e}* (CCL17-deficient) mice for co-culture with naïve CD4⁺CD62L⁺ T cells isolated from *Apoe^{-/-}*, *Apoe^{-/-}Ccr1^{-/-}* or *Apoe^{-/-}Ccr5^{-/-}* mice (**Figure 7c**). Here, we demonstrate that *Apoe^{-/-}Ccl17^{wt/e}* DCs reduce CD4⁺CD25⁺ Foxp3⁺ Treg frequencies in co-culture with T cells from *Apoe^{-/-}* or *Apoe^{-/-}Ccr5^{-/-}* mice, but not with those from *Apoe^{-/-}Ccr1^{-/-}* mice, establishing the importance of the CCL17-instructed CCL3-CCR1 axis in restraining Treg differentiation (**Figure 7d**). Accordingly, *Apoe^{-/-}Ccr1^{-/-}* mice exhibited a

decrease in lesion size and macrophage content in the aortic root and reduced lesion development in the thoraco-abdominal aorta and aortic arch (**Figure 7e-h and Supplemental Figure 6a-d**), whereas CD3⁺CD4⁺ CD25⁺Foxp3⁺ Tregs were elevated in para-aortic LNs, spleens (**Figure 7i,j**), in axillary and inguinal LNs (**Supplemental Figure 6e-g**), as compared to *Apoe*^{-/-} controls, without affecting CCL3 plasma levels (**Supplemental Figure 6h**). Plasma lipid levels, blood leukocyte and thrombocyte counts did not differ between *Apoe*^{-/-}*Ccr1*^{-/-} mice and controls (**Supplemental Table 7**). These results are in line with reduced lesion size in *Apoe*^{-/-}*Ccr1*^{-/-} mice after 4 weeks of WD.²⁹

CCL3 drives atherosclerosis and mediates reduced Treg numbers *in vivo*

When analyzing Treg frequencies under steady state conditions, we found an increase in CD4⁺ CD25⁺Foxp3⁺ Tregs among CD4⁺ T cells in para-aortic LNs and spleen (**Figure 8a-c**) as well as in axillary and inguinal LNs of *Ccl3*^{-/-} mice as compared to wild-type controls (**Supplemental Figure 6i-k**). A report by de Jager et al.³⁰ revealed a pro-atherogenic role for hematopoietic CCL3, as evidenced by protection in *Ldlr*^{-/-} mice bearing CCL3-deficient bone marrow cells. Similar to CCL17-deficient mice, *Apoe*^{-/-}*Ccl3*^{-/-} animals displayed a marked reduction in lesion size in the aortic root, thoraco-abdominal aorta and aortic arch (**Figure 8d-g**) and an increase in Treg numbers (**Figure 8h,i and Supplemental Figure 6l-n**), as compared to controls. Lesional macrophage and smooth muscle cell numbers were both reduced (**Supplemental Figure 6o-q**). Moreover, the reduction in CCL3 plasma levels was almost equivalent in CCL3 deficiency and CCL17 deficiency, corroborating the importance of CCL17 in controlling CCL3 release and Treg maintenance (**Supplemental Figure 6r**). Body weight, plasma lipid levels, and circulating leukocyte and thrombocyte counts were unaltered in *Apoe*^{-/-}*Ccl3*^{-/-} mice (**Supplemental Table 8**).

Based on our finding that CCL17 exerts its effects through interaction with CCR8 and subsequent CCL3 release, we tested whether injection of CCL3 into *Apoe*^{-/-}*Ccl17*^{+/+} mice would restore the phenotype observed in CCL17-competent mice (**Figure 8i**). Injection of CCL3 (3-times per week) into *Apoe*^{-/-}*Ccl17*^{+/+} mice during 4 weeks of WD indeed increased aortic root lesion size (**Figure 8k**) and reduced para-aortic and splenic Treg numbers to levels seen in *Apoe*^{-/-} controls (**Figure 8l,m**). Body weight, plasma lipid levels, and circulating leukocyte and thrombocyte counts did not differ between the groups (**Supplemental Table 9**). Together, our data clearly establish the importance of CCL3 in restraining Tregs and promoting atherosclerosis.

Proof-of-principle analysis in human gene expression data sets revealed increased CCL3 levels in samples from atherosclerotic carotid artery segments with advanced (thin or thick fibrous cap atheroma) as compared to early lesions (intimal thickening or xanthoma)

(**Supplemental Figure 7a**, GSE28829) or in carotid atheroma specimens (stage IV) containing plaque core and shoulders as compared to remote, macroscopically intact tissue (stages I and II) (**Supplemental Figure 7b**, GSE43292). Furthermore, we found increased CCL3 expression in human coronary arteries with atherosclerotic lesions from symptomatic as compared to asymptomatic patients with coronary artery disease (**Supplemental Figure 7c**, GSE11138). Likewise, CCL3 transcript levels were higher in atherectomy specimens of carotid artery stenosis from symptomatic patients with neuro-logical events, e.g., transient ischemic attacks (n=16), then in those from asymptomatic patients (n=13) (**Supplemental Figure 7d**). This was mirrored by reduced FoxP3 expression indicative of reduced Treg abundance in those samples (**Supplemental Figure 7e**). Furthermore, patients with familial hypercholesterolemia (FH) prone to atherosclerosis due to genetic defects in the LDL receptor (hetero- and homozygous carriers) showed a trend for reduced FoxP3 expression (**Supplemental Figure 7f**, GSE6088). Taken together, these data confirm increased CCL3 levels in progressing human lesions and imply a role in suppressing Treg differentiation in humans.

Discussion

Our quest to disambiguate the mechanisms underlying the effects of CCL17 in an atherogenic context uncovered that aortic LNs of CCL17-deficient mice contain more tolerogenic cDCs which license atheroprotective Treg maintenance. In turn, mice lacking the canonical CCL17 receptor CCR4 failed to phenocopy these effects of CCL17 deficiency on Tregs function in atherosclerosis. Instead, we were able to identify CCR8 as a new and functional high-affinity CCL17 receptor expressed by cDCs, CD4⁺ T cells and Tregs. Further analysis established that CCL17-CCR8 interaction on CD4⁺ T cells facilitates CCL3 release, thereby suppressing Treg differentiation. Accordingly, interference with CCR8 by antibody blockade or CD4⁺ T cell-specific CCR8 deletion blunted CCL3 levels and consequently atherosclerotic lesion formation. Likewise, CCL3-deficient mice displayed attenuated lesion development and increased Treg numbers, whereas CCL3 injection into CCL17-deficient mice exacerbated atherosclerosis and hampered Treg differentiation, an effect that was dependent on CCR1. We found increased CCL3 expression and reduced FoxP3 levels in human plaques as compared to healthy arteries as well as in symptomatic versus asymptomatic plaques.

CCR7 is a key receptor guiding cDCs into T-cell rich regions of lymphatic organs, enabling them to stimulate and also suppress T-cell immunity.³¹ CCR7 has also been implicated in mediating egress of antigen-presenting cells from atherosclerotic lesions.³² We have evidence that the CCR7-expressing DCs cluster in aortic LNs and harbor both CCL17⁺ and CCL17-deficient cDC populations. In the LNs from mice lacking CCL17, we found the number of CCR7-expressing DCs with a tolerogenic gene expression profile to be 2-fold higher than in controls. Hence, an increased number of tolerogenic cDCs together with locally decreased

CCL3 levels might explain the higher Treg frequency observed in lymphoid organs of CCL17-deficient mice. This is consistent with the hypothesis that CCL17⁺ DCs regulate the homeostatic mechanisms of T cells, including Treg differentiation in lymphoid tissues, and thus are able to affect the development of atherosclerosis.¹⁰ The involvement of Tregs in limiting chronic inflammation and immune responses in mouse models of atherosclerosis^{18,33} and in alleviating atherosclerosis-related diseases in humans³⁴⁻³⁶ has been widely documented.

It was remarkable that in our mouse model of atherosclerosis the deficiency of CCR4, conventionally considered as the sole CCL17 receptor, failed to recapitulate any of the experimental features associated with CCL17 deficiency. These findings mirrored related reports in experimental models of atopic dermatitis²⁰ and colitis¹¹, in which reduced inflammation was observed only in CCL17-deficient, but not in CCR4-deficient mice. Likewise, a marked discrepancy between CCR4-deficient and CCL17-deficient mice was evident in models of allograft tolerance, in which the former fail to develop tolerance due to diminished Treg recruitment, whereas the latter show prolonged allograft survival.^{13,37} Based on these findings we revisited the previously proposed but later contested concept^{24,27,38} that CCR8 may act as an alternative receptor for CCL17 and establish unequivocally that CCR8 indeed acts as a functional high-affinity receptor for CCL17. CCR8 is mainly expressed on CD4⁺ T cells and specifically on Tregs^{39,40} but its presence has also been reported on monocytes natural killer cells, group 2 innate lymphoid cells and DCs at levels dependent on disease context and tissue location.⁴¹⁻⁴³ While the role of CCR8 in cancer has received great attention⁴⁴⁻⁴⁶, reports on its contribution to chronic inflammation remain scarce. Previous studies investigated CCR8 in the context of airway inflammation⁴⁷ and established a key role of this receptor in promoting pathogenic functions of IL-5⁺ Th2 cell subset in atopic dermatitis⁴⁸. To our best knowledge, CCR8 contribution to atherosclerosis has only been addressed in one study showing that a genetic deletion of the its ligand CCL1 in *Apoe*^{-/-} mice reduced Treg recruitment to inflamed arteries and increased lesion formation.⁴⁹ The role of CCR8 was examined in *Ldlr*^{-/-} mice reconstituted with bone marrow cells expressing red fluorescent protein under the control of Foxp3. Upon treatment with a CCR8-blocking antibody, these mice displayed an increased lesion size⁴⁹, which is in apparent contrast to our findings. The experimental set-ups differed significantly, whereas Vila-Caballer *et al.* used *Ldlr*^{-/-} mice subjected to bone marrow transplantation⁴⁹, we employed *Apoe*^{-/-} mice for CCR8 blocking studies. In addition, they fed a cholesterol-rich diet for only one week, which is an unconventionally short time span to evaluate atherosclerosis and establish the pathogenic role of adaptive immune cells. Nevertheless, CCR8-expressing Tregs interacting with CCL1 have been described as key drivers of suppressive immunity in an experimental mouse model of autoimmune encephalomyelitis.²⁶ Hence, we cannot exclude that interactions of CCL1 with CCR8 driving Treg recruitment in the absence of CCL17 contribute to atheroprotective effects observed in

CCL17-deficient mice, nor can we ignore the possibility that differences in receptor affinity or local availability of its ligands shape anti- vs. pro-inflammatory immune responses mediated by CCR8. In fact, both CCR8 ligands may be involved and differential levels of production in a given pathology may determine the functional outcome.

Expression of CCR8 was initially identified on human monocytes and lymphocytes.⁵⁰ In the same study, mouse pre-B cell transfectants (4DE4) expressing CCR8 exhibited specific calcium transients in response to CCL1 but not to other chemokines tested (albeit not including CCL17), as well as migrated in response to CCL1 in a dose-dependent manner.⁵⁰ Subsequently, Bernardini et al. suggested that CCL17 can act as a functional CCR8 ligand as evident by a dose-dependent migration of CCR8-transfected Jurkat cells in response to CCL17.²⁴ This was supported by a study revealing CCR8 expression and dose-dependent migration of human IL-2-activated NK (IANK) cells in response to CCL17.³⁶ While CCL1 induced a robust CCR8-dependent calcium flux in IANK cells and partially inhibited CCL17-induced calcium flux, CCL17 fully desensitized the calcium response to CCL1. This discrepancy was explained by the expression of CCR4 on IANK cells, which cannot be desensitized by CCL1.⁴¹ Accordingly, other groups were unable to show migration, calcium flux or receptor internalization in CCR8-transfected 4DE4 cells in response to CCL17.^{38,51} This may be related to the fact that 4DE4 transfectants are a suboptimal cell model for signaling studies, whereas primary human IANK⁴¹ cells like CD4⁺ T cells used herein represent more physiological cell types expressing CCR8 (**Supplemental Figure 4b,c**). Still, calcium flux induced by CCL17 in IANK cells was predominantly mediated by CCR4.⁴¹ In light of this inconsistency, we applied assays beyond migration and receptor internalization, both of which documented CCL17 activity for CCR8, to confirm a functional high-affinity CCL17 interaction with CCR8. Proximity ligation assays in DCs or Jurkat CCR8-transfectants, SPR and CCR8 binding competition clearly revealed binding of CCL17 to CCR8 with apparent affinities ranging from 1.1 nM (K_D SPR) to 9.4 nM (IC_{50} CCL1 competition) and thus equivalent to that found for CCL18 (K_D 1.9 nM) but lower than that found for CCL1 by us (IC_{50} 0.58 nM) and others (K_i/IC_{50} 0.11-0.22 nM).^{51,52} Determining cAMP levels in CCR4- or CCR8-transfected HEK cells confirmed that CCL17 induced Gi signaling via both receptors. This extends findings that CCR8 mediates chemotactic migration in response to CCL17, unequivocally establishing that CCR8 as a signaling high-affinity receptor for CCL17. Our data can be reconciled with a report that CCL17 induced chemotaxis of Jurkat CCR8-transfectants, albeit without eliciting calcium mobilization²⁴, while findings disputing the assignment of CCL17 as a CCR8 ligand may have been due to insufficient bioactivity of the chemokine, as no positive controls were provided.²² The role of CCR8 in mediating the restraint of Treg homeostasis may thus serve to complement or counter-balance the function of CCR4 in Treg recruitment in inflammation and cancer.^{53,54} Preliminary evidence that CCR4 and CCR8 can also engage in a heterodimeric interaction

may further imply alternative mechanisms of modulation that are beyond the current scope and will be subject of future studies.

It is tempting to speculate that only chronic inflammatory conditions, as present in atherosclerosis or in atopic dermatitis²⁰ and colitis¹¹, foster the development of CCL17-expressing cDCs, which subsequently trigger Treg restraint via the induction of CCL3 release through CCR8 in lymphoid organs. Notably and surprisingly, our data show that it is primarily CCR8 on CD4⁺ T cells which orchestrates the restraint of Tregs by up-regulating CCL3 in response to CCL17 stimulation. This finding is supported by decreased lesion size and increased Treg numbers in *Apoe*^{-/-} mice lacking CCR8 on CD4⁺ T cells. Because CCR8 is prominently expressed in Tregs, it is conceivable that at sites of inflammation or in T-cell rich areas of LNs CCL17, on the one hand, directs Treg trafficking and, on the other hand, prevents further Treg differentiation through induction of CCL3. This mechanism would also explain why we found that isolated CD25⁺CD4⁺ T cells secrete CCL3 in response to CCL17. Under chronic inflammatory conditions like atherosclerosis, however, CCL17⁺ cDCs are continuously present and skewing CD4⁺ T-cell responses towards a pro-inflammatory type. This concept is corroborated by studies of immune mechanisms in psoriasis, a chronic inflammatory autoimmune disease of the skin. The transcription factor Grainyhead-like 3 is crucial for maintaining barrier integrity of the skin, while its knockdown exclusively upregulates CCL17 in keratinocytes, driving their proliferation and a strong inflammatory response with a T-cell infiltration pattern resembling psoriasis.⁵⁵ Moreover, Chen et al.⁵⁶ found that elevated CCL3 inversely correlates with FoxP3 levels in Tregs of psoriatic patients and that CCL3 interferes with FoxP3 stability by promoting ubiquitination-dependent degradation. Thus, psoriatic skin disease may also be prompted by CCL17-induced CCL3 expression to impair FoxP3 stability and reduce the number of Tregs. In future studies, it will be intriguing to dissect how much CCL3 induction by CCL17 is restricted to cell types expressing CCR8, whether additional cell types are licensed by CCR8 expression to enact this mechanism of Treg control and which specific signaling pathways couple CCR8 to CCL3 release.

Previous studies on the role of CCL3 in atherosclerosis, which notably failed to pinpoint the cellular sources of CCL3, lend support to our observations. De Jager *et al.* provided evidence that aortic lesion formation and neutrophil adhesion to inflamed endothelium was attenuated in *Ldlr*^{-/-} mice reconstituted with *Ccl3*^{-/-} bone marrow; however, the involvement of T-cell subsets was not examined.³⁰ Furthermore, administration of atorvastatin inhibited the 5-lipoxygenase pathway in *Apoe*^{-/-} mice, thereby downregulating CCL3 gene and protein expression and consequently attenuated the development of atherosclerotic lesions, also suggesting that CCL3 might be a therapeutic target in atherosclerosis.⁵⁷ Recently, mice lacking CCL3 have been found to be protected from aortic inflammation and aneurysm formation⁵⁸. In

extending these findings, we report reduced lesion size and increased Treg numbers in *Apoe*^{-/-} mice with a genetic deletion of CCL3. Turning to the CCL3 receptors CCR1 and CCR5 described, it was reported that CCR5 deficiency conferred an atheroprotective phenotype in different mouse models of atherosclerosis⁵⁹, whereas findings on CCR1 deficiency were more controversial^{29,59}. Our data clearly demonstrate that Treg restraint by CCL3 is afforded by CCR1 and that CCR1 deficiency in *Apoe*^{-/-} mice decreased lesion development and enhanced Treg numbers after 12 weeks of WD feeding. Nevertheless, findings may be reconciled depending on the mouse model and disease phenotype investigated, as CCR1 also engages many other chemokine ligands with multiple roles in immunity and inflammation. Hence, the subsets of cells closely interacting in the vicinity and the local tissue environment may determine the availability of CCR1 ligands and the way the immune response is shaped by CCL3 at relevant interfaces.

In synopsis, our data establish that CCL17, apart from ligating its canonical receptor CCR4, also binds to CCR8, its second functional high-affinity receptor. Thus, our findings introduce another chemokine, CCL17, to the unique ligand spectrum of CCR8, which, in addition, includes its major ligand CCL1, CCL8⁴⁸, a chemokine responsible for the pathogenic circuits in atopic dermatitis as well as a widely expressed inflammatory chemokine CCL18.⁵¹ The functional relevance in primary cells, i.e. Tregs, uncovers yet another facet to the remarkable versatility of the chemokine-receptor family.⁶⁰ Our data further show that CCL17 signaling via CCR8 on CD4⁺ T cells triggers their secretion of CCL3, which, in turn, suppresses Treg differentiation in a CCR1-dependent manner to drive proatherogenic effects of CCL17 (**Supplemental Figure 8**). We suggest that the specific instruction of CD4⁺ T cells by CCL17⁺ cDCs dictating the CCL3-dependent restraint of Tregs may constitute a novel, broadly relevant mechanism in chronic inflammatory diseases and put forward the sequential CCL17-CCR8-CCL3-CCR1 molecular pathway as an attractive potential target for multilayered therapeutic interventions in these diseases.

References

- 1 Lutgens, E. *et al.* Immunotherapy for cardiovascular disease. *Eur Heart J* **40**, 3937-3946, doi:10.1093/eurheartj/ehz283 (2019).
- 2 Jongstra-Bilen, J. *et al.* Low-grade chronic inflammation in regions of the normal mouse arterial intima predisposed to atherosclerosis. *J Exp Med* **203**, 2073-2083, doi:10.1084/jem.20060245 (2006).
- 3 Millonig, G. *et al.* Network of vascular-associated dendritic cells in intima of healthy young individuals. *Arterioscler Thromb Vasc Biol* **21**, 503-508, doi:10.1161/01.atv.21.4.503 (2001).
- 4 Choi, J. H. *et al.* Identification of antigen-presenting dendritic cells in mouse aorta and cardiac valves. *J Exp Med* **206**, 497-505, doi:10.1084/jem.20082129 (2009).
- 5 Gil-Pulido, J. & Zernecke, A. Antigen-presenting dendritic cells in atherosclerosis. *Eur J Pharmacol* **816**, 25-31, doi:10.1016/j.ejphar.2017.08.016 (2017).
- 6 Ye, Y. *et al.* Serum chemokine CCL17/thymus activation and regulated chemokine is correlated with coronary artery diseases. *Atherosclerosis* **238**, 365-369, doi:10.1016/j.atherosclerosis.2014.12.047 (2015).
- 7 Brunner, P. M. *et al.* The atopic dermatitis blood signature is characterized by increases in inflammatory and cardiovascular risk proteins. *Sci Rep* **7**, 8707, doi:10.1038/s41598-017-09207-z (2017).
- 8 He, H. *et al.* Increased cardiovascular and atherosclerosis markers in blood of older patients with atopic dermatitis. *Ann Allergy Asthma Immunol* **124**, 70-78, doi:10.1016/j.anai.2019.10.013 (2020).
- 9 Ye, Y. *et al.* Association Between a CCL17 Genetic Variant and Risk of Coronary Artery Disease in a Chinese Han Population. *Circ J* **82**, 224-231, doi:10.1253/circj.CJ-17-0190 (2017).
- 10 Weber, C. *et al.* CCL17-expressing dendritic cells drive atherosclerosis by restraining regulatory T cell homeostasis in mice. *J Clin Invest* **121**, 2898-2910, doi:10.1172/JCI44925 (2011).
- 11 Heiseke, A. F. *et al.* CCL17 promotes intestinal inflammation in mice and counteracts regulatory T cell-mediated protection from colitis. *Gastroenterology* **142**, 335-345, doi:10.1053/j.gastro.2011.10.027 (2012).
- 12 Steinman, R. M. Decisions about dendritic cells: past, present, and future. *Annu Rev Immunol* **30**, 1-22, doi:10.1146/annurev-immunol-100311-102839 (2012).
- 13 Alferink, J. *et al.* Compartmentalized production of CCL17 in vivo: strong inducibility in peripheral dendritic cells contrasts selective absence from the spleen. *J Exp Med* **197**, 585-599 (2003).
- 14 Ali, A. J., Makings, J. & Ley, K. Regulatory T Cell Stability and Plasticity in Atherosclerosis. *Cells* **9**, doi:10.3390/cells9122665 (2020).
- 15 Saigusa, R., Winkels, H. & Ley, K. T cell subsets and functions in atherosclerosis. *Nat Rev Cardiol* **17**, 387-401, doi:10.1038/s41569-020-0352-5 (2020).
- 16 Arce-Sillas, A. *et al.* Regulatory T Cells: Molecular Actions on Effector Cells in Immune Regulation. *J Immunol Res* **2016**, 1720827, doi:10.1155/2016/1720827 (2016).
- 17 Sharma, M. *et al.* Regulatory T Cells License Macrophage Pro-Resolving Functions During Atherosclerosis Regression. *Circulation research* **127**, 335-353, doi:10.1161/CIRCRESAHA.119.316461 (2020).
- 18 Ait-Oufella, H. *et al.* Natural regulatory T cells control the development of atherosclerosis in mice. *Nat Med* **12**, 178-180, doi:10.1038/nm1343 (2006).
- 19 Imai, T. *et al.* The T cell-directed CC chemokine TARC is a highly specific biological ligand for CC chemokine receptor 4. *The Journal of biological chemistry* **272**, 15036-15042, doi:10.1074/jbc.272.23.15036 (1997).
- 20 Stutte, S. *et al.* Requirement of CCL17 for CCR7- and CXCR4-dependent migration of cutaneous dendritic cells. *Proc Natl Acad Sci U S A* **107**, 8736-8741, doi:10.1073/pnas.0906126107 (2010).
- 21 Wild, A. B. *et al.* CD83 orchestrates immunity toward self and non-self in dendritic cells. *JCI Insight* **4**, doi:10.1172/jci.insight.126246 (2019).
- 22 Wan, W., Lionakis, M. S., Liu, Q., Roffe, E. & Murphy, P. M. Genetic deletion of chemokine receptor Ccr7 exacerbates atherogenesis in ApoE-deficient mice. *Cardiovasc Res* **97**, 580-588, doi:10.1093/cvr/cvs349 (2013).
- 23 Luchtefeld, M. *et al.* Chemokine receptor 7 knockout attenuates atherosclerotic plaque development. *Circulation* **122**, 1621-1628, doi:10.1161/CIRCULATIONAHA.110.956730 (2010).

- 24 Bernardini, G. *et al.* Identification of the CC chemokines TARC and macrophage inflammatory protein-1 beta as novel functional ligands for the CCR8 receptor. *Eur J Immunol* **28**, 582-588, doi:10.1002/(SICI)1521-4141(199802)28:02<582::AID-IMMU582>3.0.CO;2-A (1998).
- 25 Garlisi, C. G. *et al.* The assignment of chemokine-chemokine receptor pairs: TARC and MIP-1 beta are not ligands for human CC-chemokine receptor 8. *Eur J Immunol* **29**, 3210-3215, doi:10.1002/(SICI)1521-4141(199910)29:10<3210::AID-IMMU3210>3.0.CO;2-W (1999).
- 26 Barsheshet, Y. *et al.* CCR8(+)FOXP3(+) Treg cells as master drivers of immune regulation. *Proc Natl Acad Sci U S A* **114**, 6086-6091, doi:10.1073/pnas.1621280114 (2017).
- 27 Iellem, A. *et al.* Unique chemotactic response profile and specific expression of chemokine receptors CCR4 and CCR8 by CD4(+)CD25(+) regulatory T cells. *J Exp Med* **194**, 847-853, doi:10.1084/jem.194.6.847 (2001).
- 28 Li, J. *et al.* CCR5+T-bet+FoxP3+ Effector CD4 T Cells Drive Atherosclerosis. *Circulation research* **118**, 1540-1552, doi:10.1161/CIRCRESAHA.116.308648 (2016).
- 29 Soehnlein, O. *et al.* Distinct functions of chemokine receptor axes in the atherogenic mobilization and recruitment of classical monocytes. *EMBO Mol Med* **5**, 471-481, doi:10.1002/emmm.201201717 (2013).
- 30 de Jager, S. C. *et al.* Leukocyte-specific CCL3 deficiency inhibits atherosclerotic lesion development by affecting neutrophil accumulation. *Arterioscler Thromb Vasc Biol* **33**, e75-83, doi:10.1161/ATVBAHA.112.300857 (2013).
- 31 Schneider, M. A., Meingassner, J. G., Lipp, M., Moore, H. D. & Rot, A. CCR7 is required for the in vivo function of CD4+ CD25+ regulatory T cells. *J Exp Med* **204**, 735-745, doi:10.1084/jem.20061405 (2007).
- 32 Worbs, T., Hammerschmidt, S. I. & Forster, R. Dendritic cell migration in health and disease. *Nat Rev Immunol* **17**, 30-48, doi:10.1038/nri.2016.116 (2017).
- 33 Klingenberg, R. *et al.* Depletion of FOXP3+ regulatory T cells promotes hypercholesterolemia and atherosclerosis. *J Clin Invest* **123**, 1323-1334, doi:10.1172/JCI63891 (2013).
- 34 Mor, A., Luboshits, G., Planer, D., Keren, G. & George, J. Altered status of CD4(+)CD25(+) regulatory T cells in patients with acute coronary syndromes. *Eur Heart J* **27**, 2530-2537, doi:10.1093/eurheartj/ehl222 (2006).
- 35 Zhang, W. C. *et al.* Impaired thymic export and increased apoptosis account for regulatory T cell defects in patients with non-ST segment elevation acute coronary syndrome. *The Journal of biological chemistry* **287**, 34157-34166, doi:10.1074/jbc.M112.382978 (2012).
- 36 Albany, C. J., Trevelin, S. C., Giganti, G., Lombardi, G. & Scotta, C. Getting to the Heart of the Matter: The Role of Regulatory T-Cells (Tregs) in Cardiovascular Disease (CVD) and Atherosclerosis. *Front Immunol* **10**, 2795, doi:10.3389/fimmu.2019.02795 (2019).
- 37 Lee, I. *et al.* Recruitment of Foxp3+ T regulatory cells mediating allograft tolerance depends on the CCR4 chemokine receptor. *J Exp Med* **201**, 1037-1044, doi:10.1084/jem.20041709 (2005).
- 38 Fox, J. M. *et al.* Structure/function relationships of CCR8 agonists and antagonists. Amino-terminal extension of CCL1 by a single amino acid generates a partial agonist. *The Journal of biological chemistry* **281**, 36652-36661, doi:10.1074/jbc.M605584200 (2006).
- 39 Freeman, C. M. *et al.* CCR8 is expressed by antigen-elicited, IL-10-producing CD4+CD25+ T cells, which regulate Th2-mediated granuloma formation in mice. *Journal of immunology* **174**, 1962-1970, doi:10.4049/jimmunol.174.4.1962 (2005).
- 40 Sebastiani, S. *et al.* Chemokine receptor expression and function in CD4+ T lymphocytes with regulatory activity. *Journal of immunology* **166**, 996-1002, doi:10.4049/jimmunol.166.2.996 (2001).
- 41 Inngjerdingen, M., Damaj, B. & Maghazachi, A. A. Human NK cells express CC chemokine receptors 4 and 8 and respond to thymus and activation-regulated chemokine, macrophage-derived chemokine, and I-309. *Journal of immunology* **164**, 4048-4054, doi:10.4049/jimmunol.164.8.4048 (2000).
- 42 Puttur, F. *et al.* Pulmonary environmental cues drive group 2 innate lymphoid cell dynamics in mice and humans. *Science immunology* **4**, doi:10.1126/sciimmunol.aav7638 (2019).
- 43 Sokol, C. L., Camire, R. B., Jones, M. C. & Luster, A. D. The Chemokine Receptor CCR8 Promotes the Migration of Dendritic Cells into the Lymph Node Parenchyma to Initiate the Allergic Immune Response. *Immunity* **49**, 449-463 e446, doi:10.1016/j.immuni.2018.07.012 (2018).
- 44 De Simone, M. *et al.* Transcriptional Landscape of Human Tissue Lymphocytes Unveils Uniqueness of Tumor-Infiltrating T Regulatory Cells. *Immunity* **45**, 1135-1147,

- doi:10.1016/j.immuni.2016.10.021 (2016).
- 45 Eruslanov, E. *et al.* Expansion of CCR8(+) inflammatory myeloid cells in cancer patients with urothelial and renal carcinomas. *Clin Cancer Res* **19**, 1670-1680, doi:10.1158/1078-0432.CCR-12-2091 (2013).
 - 46 Villarreal, D. O. *et al.* Targeting CCR8 Induces Protective Antitumor Immunity and Enhances Vaccine-Induced Responses in Colon Cancer. *Cancer research* **78**, 5340-5348, doi:10.1158/0008-5472.CAN-18-1119 (2018).
 - 47 Mitsuyama, E., Kunori, Y., Kamimura, T. & Kaminuma, O. Functional chemokine receptors in allergic diseases: is CCR8 a novel therapeutic target? *Mini Rev Med Chem* **6**, 463-466, doi:10.2174/138955706776361394 (2006).
 - 48 Islam, S. A. *et al.* Mouse CCL8, a CCR8 agonist, promotes atopic dermatitis by recruiting IL-5+ T(H)2 cells. *Nat Immunol* **12**, 167-177, doi:10.1038/ni.1984 (2011).
 - 49 Vila-Caballer, M. *et al.* Disruption of the CCL1-CCR8 axis inhibits vascular Treg recruitment and function and promotes atherosclerosis in mice. *J Mol Cell Cardiol* **132**, 154-163, doi:10.1016/j.yjmcc.2019.05.009 (2019).
 - 50 Tiffany, H. L. *et al.* Identification of CCR8: a human monocyte and thymus receptor for the CC chemokine I-309. *J Exp Med* **186**, 165-170, doi:10.1084/jem.186.1.165 (1997).
 - 51 Islam, S. A., Ling, M. F., Leung, J., Shreffler, W. G. & Luster, A. D. Identification of human CCR8 as a CCL18 receptor. *J Exp Med* **210**, 1889-1898, doi:10.1084/jem.20130240 (2013).
 - 52 Liu, L. *et al.* Biological characterization of ligands targeting the human CC chemokine receptor 8 (CCR8) reveals the biased signaling properties of small molecule agonists. *Biochem Pharmacol* **188**, 114565, doi:10.1016/j.bcp.2021.114565 (2021).
 - 53 Haas, J. *et al.* Specific recruitment of regulatory T cells into the CSF in lymphomatous and carcinomatous meningitis. *Blood* **111**, 761-766, doi:10.1182/blood-2007-08-104877 (2008).
 - 54 Oo, Y. H. *et al.* Distinct roles for CCR4 and CXCR3 in the recruitment and positioning of regulatory T cells in the inflamed human liver. *Journal of immunology* **184**, 2886-2898, doi:10.4049/jimmunol.0901216 (2010).
 - 55 Goldie, S. J. *et al.* Loss of GRHL3 leads to TARC/CCL17-mediated keratinocyte proliferation in the epidermis. *Cell Death Dis* **9**, 1072, doi:10.1038/s41419-018-0901-6 (2018).
 - 56 Chen, L., Wu, J., Pier, E., Zhao, Y. & Shen, Z. mTORC2-PKBalpha/Akt1 Serine 473 phosphorylation axis is essential for regulation of FOXP3 Stability by chemokine CCL3 in psoriasis. *J Invest Dermatol* **133**, 418-428, doi:10.1038/jid.2012.333 (2013).
 - 57 Yang, L.-X. *et al.* Atorvastatin inhibits the 5-lipoxygenase pathway and expression of CCL3 to alleviate atherosclerotic lesions in atherosclerotic ApoE knockout mice. *J. Cardiovasc. Pharmacol.* **62**, 205-211, doi:10.1097/FJC.0b013e3182967fc0 (2013).
 - 58 Ishida, Y. *et al.* Prevention of CaCl₂-induced aortic inflammation and subsequent aneurysm formation by the CCL3-CCR5 axis. *Nat Commun* **11**, 5994, doi:10.1038/s41467-020-19763-0 (2020).
 - 59 Braunersreuther, V. *et al.* Ccr5 but not Ccr1 deficiency reduces development of diet-induced atherosclerosis in mice. *Arterioscler. Thromb. Vasc. Biol.* **27**, 373-379, doi:10.1161/01.ATV.0000253886.44609.ae (2007).
 - 60 Bachelier, F. *et al.* International Union of Basic and Clinical Pharmacology. [corrected]. LXXXIX. Update on the extended family of chemokine receptors and introducing a new nomenclature for atypical chemokine receptors. *Pharmacol Rev* **66**, 1-79, doi:10.1124/pr.113.007724 (2014).

Funding

This work was supported by Deutsche Forschungsgemeinschaft (DFG) SFB1123-A1/A10 to Y.D. and C.W., SFB1123-A2 to P.v.H., SFB1123-B1 to D.T. and L.H., by the European Research Council (ERC AdG °692511 to C.W.), by the DZHK (German Centre for Cardiovascular Research) and the BMBF (German Ministry of Education and Research) to Y.D., C.W. and E.P.C.v.d.V., by grants from the Interdisciplinary Center for Clinical Research within the faculty of Medicine at the RWTH Aachen University and NWO-ZonMw Veni (91619053) to E.P.C.v.d.V.,

by the DFG YI 133/3-5 and Friedrich-Baur-Stiftung 39/20, to C.Y.; by the DFG HA 1083/15-4, HA 1083/15-5 and ERA-CVD (PLAQUEFIGHT) 01KL1808 to A.J.R.H.

Acknowledgments

We are indebted to Antal Rot for thoughtful discussions and thorough review of the manuscript. We thank Olga Schengel and animal facility for excellent technical assistance. We thank Stefanos Michaelides (LMU Munich) for generously providing Jurkat CCR4 and CCR8 transfectants, Klaus Pfeffer (Heinrich-Heine-Universität, Düsseldorf, Germany) for kindly providing *Ccr4*^{-/-} mice, and Irmgard Förster (Universität Bonn, Germany) for generously providing *Ccl17*^{+/e} (GFP reporter knock-in) mice.

Author Contributions

Y.D. conceived and supervised the study, designed experiments, provided funding performed experiments, analyzed data, and wrote the manuscript. E.v.d.V. supervised the study, designed experiments, performed experiments, analyzed data, and contributed to writing the manuscript. Y.Y. and C.N. designed experiments, performed experiments and analyzed the data. Y.J. performed and analyzed mouse experiments and data. X.B. and J.L. performed and analyzed plasmon resonance and receptor binding assays, M.M., L.F.J. and S.G. contributed to conduction of mouse experiments and data analysis. M.H. performed cell sorting experiments, C.Y., X.Z. and A.H. contributed to single cell RNA sequencing experiments and data analysis. A.F. helped performing and analyzing cAMP signaling assays and provided critical reagents, D.T. and L.H. provided human plaque material and analysis. C.M. and I.P. provided critical reagents, contributed to single cell RNA sequencing experiments and data analysis and provided intellectual input. P.v.H. critically contributed to receptor binding experiments, analyzed data, provided supervision and intellectual input, and contributed to writing the manuscript. C.W. conceived and supervised the study, designed experiments, provided funding, and wrote the manuscript.

Competing Financial Interests

The authors declare no competing financial interests.

Online content, data and materials availability

Materials and Methods including experimental details and reagents can be found in the Supplementary Materials. All data associated with this study are present in the main text or the Supplementary Materials. RNAseq data sets are available upon request.

Figure 1. CCR4 does not affect atherosclerosis or Tregs, while CCL17-deficiency increases tolerogenic DCs.

(a) Experimental scheme of Western diet (WD) feeding for 12 weeks; **(b)** Representative sections and quantification of lesion area measured after Oil-Red-O staining for lipid deposits in the aortic root of *Apoe*^{-/-} or *Apoe*^{-/-} *Ccr4*^{-/-} mice (n=16-20). Scale bar = 500 μm; **(c)** Quantification of lesion area measured after Oil-Red-O staining for lipid deposits in the thoraco-abdominal aorta of *Apoe*^{-/-} or *Apoe*^{-/-} *Ccr4*^{-/-} mice (n=15-17); **(d)** Atherosclerotic lesion size in aortic arches, quantified by H&E staining of *Apoe*^{-/-} or *Apoe*^{-/-} *Ccr4*^{-/-} mice (n=15-20); **(e,f)** Representative dot plots and flow cytometric quantification of CD45⁺CD3⁺CD4⁺CD25⁺FoxP3⁺ Tregs in para-aortic lymph nodes (LNs) (n=16-20) **(e)** and in spleen (n=16-20) **(f)**; **(g)** Co-culture of CD45⁺CD11c⁺MHCII⁺ DCs sorted from *Apoe*^{-/-}, *Apoe*^{-/-} *Ccl17*^{+/e} or *Apoe*^{-/-} *Ccr4*^{-/-} mice with splenic CD4⁺CD62L⁺ T cells isolated from *Apoe*^{-/-} mice. After 72h, the abundance of CD45⁺CD3⁺CD4⁺CD25⁺FoxP3⁺ Tregs was determined by flow cytometry (n=4-7); **(h-j)** Viable CD45⁺CD3⁻CD11c⁺ cells were sorted from pooled LNs of *Apoe*^{-/-} *Ccl17*^{wt/e} or *Apoe*^{-/-} *Ccl17*^{e/e} mice (n=6-8) on chow diet. **(h)** UMAP projection of 4731 single cells colored by inferred cell types consisting of 7 distinct dendritic cell (DC) clusters **(i)** Depicted are eGFP⁺ cell counts in CCR7⁺ DCs or other DCs (percentage of total numbers) and proportions of 4 distinct CCR7⁺ DC clusters among all single cells (CD45⁺CD3⁻CD11c⁺) (bottom). **(j)** A tolerogenic score was calculated for 4 distinct DC clusters and other DC clusters based on the top 20 genes differentially expressed between tolerogenic and immunogenic DCs (top). Tolerogenic score = [1 + mean (top 20 upregulated tolerogenic genes)]/[1 + mean(top 20 upregulated immunogenic genes)]. Cell counts of four CCR7⁺ DC clusters and other DC clusters are given in the table (bottom). **(a-g)** Data represent mean±SEM. **P*<0.05; ***P*<0.01; ****P*<0.001, as analyzed by Kruskal-Wallis with Dunn's comparisons test.

Figure 2. CCL3 induction by CCL17 does not require CCR4 but inversely correlates with Treg numbers.

(a) Experimental scheme of Western diet (WD) feeding for 12 weeks in *Apoe*^{-/-}, *Apoe*^{-/-}*Ccl17*^{o/e} and *Apoe*^{-/-}*Ccr4*^{-/-} mice; **(b,c)** CCL3 plasma concentrations in *Apoe*^{-/-}*Ccl17*^{o/e} and *Apoe*^{-/-} mice (n=18-21) **(b)** or *Apoe*^{-/-}*Ccr4*^{-/-} and *Apoe*^{-/-} mice (n=25) **(c)**, as measured by ELISA; **(d)** Experimental scheme of reconstituting irradiated *Apoe*^{-/-} or *Apoe*^{-/-}*Ccl17*^{o/e} mice with *Apoe*^{-/-} bone marrow before feeding a WD for 12 weeks; **(e)** CCL3 concentrations in plasma of *Apoe*^{-/-} ► *Apoe*^{-/-} or *Apoe*^{-/-} ► *Apoe*^{-/-} *Ccl17*^{o/e} mice were measured by ELISA (n=5); **(f)** Sorted CD11c⁺MHCII⁺ conventional DCs (cDCs), CD3⁺ T cells or CD19⁺ B220⁺ B cells from lymph nodes (LNs), isolated CD115⁺ monocytes and Ly6G⁺ neutrophils from spleen and bone marrow were cultured for 4h in the presence or absence of recombinant mouse CCL17. CCL3 concentrations in the supernatant were measured by multiplex-bead-array (n=3-11); **(g)** Isolated T-cell subsets from LN suspensions of *Apoe*^{-/-} mice were stimulated for 4h in the presence or absence of CCL17. CCL3 concentrations in supernatants are measured by ELISA (n=5-6); **(h)** Sorted CD11c⁺MHCII⁺eGFP⁻ cDCs (CCL17-competent) or CD11c⁺MHCII⁺ eGFP⁺ cDCs (CCL17-deficient) from *Apoe*^{-/-}*Ccl17*^{o/WT} mice are cultured for 4h in the presence or absence of CCL17. CCL3 concentrations in supernatants were measured by ELISA (n=7-11); **(i)** Sorted CD11c⁺MHCII⁺ cDCs from LNs of *Apoe*^{-/-} mice were cultured for 4h in the presence or absence of CCL17 with or without the CCR4 inhibitor C021, and CCL3 concentrations in supernatants of isolated cDCs were measured by multiplex-bead-array (n=6); **(j)** Isolated T-cell subsets from LN suspensions of *Apoe*^{-/-} mice were stimulated with or without CCL17 in the presence or absence of the CCR4 inhibitor C021 for 4h, and CCL3 concentrations in supernatants were measured by ELISA (n=4-5). **(b-j)** Data represent mean±SEM. #**P*<0.05; ***P*<0.01; ****P*<0.001 versus control/*Apoe*^{-/-}, as analyzed by Student's t-test with Welch correction, Mann-Whitney or Kruskal-Wallis with Dunn's comparisons test as appropriate.

Figure 3. CCL17 binds to CCR8 with high affinity in the human and mouse cells.

(a) Surface plasmon resonance (SPR) to detect CCL17 interactions. Biotinylated human CCL17 was immobilized on neutravidin-modified C1 sensor chips and sensorgrams of human CCR8-, CCR4-, mock protein-carrying or pure liposomes perfused as indicated (all at 0.5 $\mu\text{g/ml}$) were recorded using a Biacore X100 instrument. **(b)** Binding kinetics of CCR8-carrying liposomes perfused at indicated concentrations on immobilized CCL17 were determined after fitting (red) of curves (blue traces) with a 1:1 interaction model (Langmuir). Concentration-independent dissociation was low (k_{off} $4.2 \pm 0.8/\text{s}$, $n=5$), indicating high stability of the complex. Calculating the ratio from k_{off} and k_{on} using the theoretical molecular weight of human CCR8 of 40.2 kD resulted in an apparent K_D of 1.1 ± 0.4 nM. Shown is one of 5 representative experiments. RU = response units. **(c)** Saturation binding of a representative experiment from **(b)** was fitted with one-site specific binding and calculated with the same molecular weight, yielding a K_D of 7.8 nM, RU = response units. **(d,e)** Interactions between mouse CCL17 or CCL1 with CCR4 and CCR8 were analyzed in stably transfected Jurkat cells using the Duolink proximity ligation assay. Signals generated by close proximity of antibodies bound to ligands and receptors on the surface of CCR8- **(d)** or CCR4-transfectants **(e)** reacted with non-blocking antibodies, as indicated, were quantified by flow cytometry ($n=3$ in duplicate). For anti-CCL17 and anti-CCL1 incubation, recombinant CCL17 (100 ng/ml) or CCL1 (50 ng/ml) were added, respectively. Data represent mean \pm SEM. * $P < 0.05$ as analyzed by Kruskal-Wallis with Dunn's multiple comparisons test. **(f,g)** HEK293 cells stably transfected with human CCR8 were incubated with CCL1 or CCL17 labeled with Alexa-Fluor 647 (AF467) at the C-terminus (20 nM each). Background binding to mock HEK293 cells was subtracted and data were normalized to binding without unlabeled chemokine (control) and subjected to nonlinear fitting. Shown is one representative of four experiments performed in triplicate. **(f)** Inhibition of CCL17^{AF647} binding to CCR8-transfectants with increasing concentrations of unlabeled CCL1; IC_{50} 0.58 nM. **(g)** Inhibition of CCL1^{AF647} binding to CCR8-transfectants with increasing concentrations of unlabeled CCL17; IC_{50} 9.4 nM. **(h,i)** Representative histogram and quantification of CCR8 surface availability and internalization upon stimulation with recombinant mouse CCL17 (100 ng/ml) on CD4⁺ T cells isolated from thymus **(f)**, $n=5-6$ and lymph nodes **(g)**, $n=5$ from CCR8^{WT}ApoE^{-/-} or CCR8^{KO}ApoE^{-/-} mice. **(j,k)** Representative histogram and quantification of CCR8 **(i)**, $n=6-12$ and CCR4 **(j)**, $n=6-12$ surface availability and internalization upon stimulation with recombinant human CCL17 (100 ng/ml), CCL1 (50 ng/ml) and CCL22 (50 ng/ml) on CD4⁺ T cells isolated from human PBMCs. Data represent mean \pm SEM. * $P < 0.05$; ** $P < 0.001$; *** $P < 0.0001$ compared to unstimulated control, as analyzed by Kruskal-Wallis with Dunn's multiple comparisons test.

Figure 4. CCL17-CCR8 interaction induces G-protein-coupled signaling and T-cell chemotaxis.

(a,b) Glosensor-HEK293 cells transfected with either CCR4 **(a)** or CCR8 **(b)**. Cells were stimulated with recombinant human CCL17, CCL1, CCL20 (all 100 ng/ml) or PBS as vehicle control after 25 min of equilibration. Shown is one of 4 representative experiments. **(c)** Transwell migration of CD4⁺ T cells isolated from *CCR8^{WT} Apoe^{-/-}* or *CCR8^{KO} Apoe^{-/-}* mice towards recombinant murine chemokines. Migrated cells were quantified by flow cytometry, chemotactic index induced by the chemokines CCL17 (100 ng/ml), CCL1 (50 ng/ml) and CCL22 (50 ng/ml) was calculated as the ratio of chemokine-stimulated to unstimulated migration (n=5-8); **(d)** Transwell migration of CD4⁺ T cells isolated from *CCR8^{WT} Apoe^{-/-}* or *CCR8^{KO} Apoe^{-/-}* mice towards recombinant murine CCL17 displayed in a checkerboard heatmap format; columns indicate CCL17 concentrations (ng/ml) in the upper chamber, rows indicate CCL17 concentrations (ng/ml) in the lower chamber. While blue represents enhanced, grey indicates reduced migration towards CCL17 in the bottom chamber. Each box represents a mean value of 3 independent experiments. **(c,d)** Data represent mean±SEM. **P*<0.05; ***P*<0.01 versus *CCR8^{WT} Apoe^{-/-}*, as analyzed by Student's t-test with Welch correction or Mann-Whitney test as appropriate.

Figure 5. CCL17-CCR8 –CCL3 axis critically interferes with Treg differentiation.

(a) Scheme of co-culture experiment, where isolated splenic CD4⁺CD62L⁺ T cells from *CCR8^{WT} Apoe^{-/-}* or *CCR8^{KO} Apoe^{-/-}* mice were combined with sorted CD11c⁺MHCII⁺ cDCs from LN of *CCR8^{WT} Apoe^{-/-}* mice and cultured for 3 days in absence or presence of recombinant murine CCL17 (100 ng/ml). **(b)** CCL3 concentrations were measured in cell supernatants by ELISA; **(c)** CD4⁺CD25⁺Foxp3⁺ Tregs were quantified using flow cytometry analysis; **(d)** Scheme of co-culture experiment, where isolated splenic CD4⁺CD62L⁺ T cells from *CCR8^{WT} Apoe^{-/-}* or *CCR8^{KO} Apoe^{-/-}* mice were combined with sorted CD11c⁺MHCII⁺ cDCs from LN of *Apoe^{-/-}* or *Apoe^{-/-} Ccl17^{oe/e}* mice and cultured for 3 days. **(e)** CCL3 concentrations in the supernatant were determined by ELISA; **(f)** CD4⁺CD25⁺Foxp3⁺ Tregs were quantified by flow cytometry; **(g)** Scheme of co-culture experiment, where splenic CD4⁺CD62L⁺ T cells isolated from *Apoe^{-/-}* or *Apoe^{-/-} Ccl3^{-/-}* mice were combined with sorted CD11c⁺MHCII⁺ cDCs from LN of *Apoe^{-/-}* mice and cultured for 3 days; **(h)** CCL3 concentrations in the supernatant were determined by ELISA; **(i)** CD4⁺CD25⁺Foxp3⁺ Tregs were quantified by flow cytometry. **(a-i)** All data were obtained from n=4-7 independent experiments with 2-5 replicates each and represent mean±SEM. **P*<0.05; ***P*<0.01; ****P*<0.001, as analyzed by Kruskal-Wallis with Dunn's multiple comparisons test.

Figure 6. Blocking CCR8 or CD4⁺ T cell-specific CCR8 deficiency reduce atherosclerosis and increase Tregs.

(a) Experimental scheme of *Apoe*^{-/-} mice fed a Western diet (WD) and injected 3x weekly with a blocking antibody to CCR8 or isotype control for 4 weeks. **(b)** Representative images and quantification of atherosclerotic lesion size in aortic arches of *Apoe*^{-/-} mice. using H&E staining (n=8-9). **(c)** Lesion area measured after Oil-Red-O staining for lipid deposits in the aortic root of *Apoe*^{-/-} mice (n=9-10). Scale bar = 500 μ m. **(d)** CCL3 mRNA expression levels in LNs of *Apoe*^{-/-} mice. 18sRNA was used as a housekeeping gene and changes in expression are given as fold change calculated with the $2^{-\Delta\Delta Ct}$ method (n=9-10); **(e, f)** Flow cytometric quantification of CD45⁺CD3⁺CD4⁺CD25⁺FoxP3⁺Tregs in para-aortic LNs (n=9-10) **(e)** and spleens (n=8) **(f)** of *Apoe*^{-/-} mice; **(g)** Experimental scheme of *Apoe*^{-/-} *CD4*^{Cre-} *Ccr8*^{WT} or *Apoe*^{-/-} *CD4*^{Cre+} *Ccr8*^{KO} mice fed a WD for 12 weeks **(h-l)**. **(h)** Representative images and quantification of lesion area in the aortic arches of *Apoe*^{-/-} *CD4*^{Cre-} *Ccr8*^{WT} or *Apoe*^{-/-} *CD4*^{Cre+} *Ccr8*^{KO} mice (n=19-22) after HE staining. **(i)** Atherosclerotic lesion size in aortas of *Apoe*^{-/-} *CD4*^{Cre-} *Ccr8*^{WT} or *Apoe*^{-/-} *CD4*^{Cre+} *Ccr8*^{KO} mice (n=19-22), as quantified by Oil-Red-O staining; **(j)** CCL3 mRNA expression levels in LNs of *Apoe*^{-/-} *CD4*^{Cre-} *Ccr8*^{WT} or *Apoe*^{-/-} *CD4*^{Cre+} *Ccr8*^{KO} mice. 18sRNA was used as a housekeeping gene and changes in expression are given as fold change calculated with the $2^{-\Delta\Delta Ct}$ method (n=16-19); **(k, l)** Flow cytometric quantification of CD45⁺CD3⁺CD4⁺CD25⁺FoxP3⁺Tregs in para-aortic LNs (n=19-22) **(k)** and spleen (n=19-22) **(l)** of *Apoe*^{-/-} *CD4*^{Cre-} *Ccr8*^{WT} or *Apoe*^{-/-} *CD4*^{Cre+} *Ccr8*^{KO} mice. **(a-l)** Data represent mean \pm SEM. **P*<0.05; ***P*<0.01, as analyzed by Student's t-test with Welch correction or Mann-Whitney test, as appropriate.

Figure 7. CCL3 released in a CCL17-dependent manner controls Treg differentiation via CCR1.

(a) Experimental scheme wherein CD4⁺CD62L⁺ T cells isolated from spleens of *Apoe*^{-/-}, *Apoe*^{-/-}*Ccr1*^{-/-} or *Apoe*^{-/-}*Ccr5*^{-/-} mice were cultured for 3 days under Treg-polarizing conditions (100 ng/ml TGFβ) in the presence or absence of recombinant mouse CCL3 (100 ng/ml). **(b)** Quantification of CD45⁺CD4⁺CD25⁺Foxp3⁺ Tregs (n=6-8) using flow cytometry. **(c)** Scheme of co-culture experiment wherein CD4⁺CD62L⁺ T cells isolated from spleens of *Apoe*^{-/-}, *Apoe*^{-/-}*Ccr1*^{-/-} or *Apoe*^{-/-}*Ccr5*^{-/-} mice were combined with sorted CD45⁺CD11c⁺MHCII⁺eGFP⁺ cDCs from LN of *Apoe*^{-/-}*Ccl17*^{wt/e} or *Apoe*^{-/-}*Ccl17*^{e/e} mice and cultured for 3 days. **(d)** Quantification of CD45⁺CD4⁺CD25⁺Foxp3⁺ Tregs (n=5-6) using flow cytometry. **(e)** Experimental scheme of *Apoe*^{-/-} or *Apoe*^{-/-}*Ccr1*^{-/-} mice fed a WD for 12 weeks **(e-j)**. **(f)** Representative images and quantification of lesion area after Oil-Red-O staining for lipid deposits in the aortic root of *Apoe*^{-/-} or *Apoe*^{-/-}*Ccr1*^{-/-} mice (n=9-12). Scale bar = 500μm. **(g)** Quantification of lesion area after Oil-Red-O staining for lipid deposits in the thoraco-abdominal aorta of *Apoe*^{-/-} or *Apoe*^{-/-}*Ccr1*^{-/-} mice (n=8-11). **(h)** Representative images and quantification of atherosclerotic lesion size in aortic arches after H&E staining (n = 8-10). **(i, j)** Flow cytometric quantification of CD45⁺CD3⁺CD4⁺CD25⁺FoxP3⁺ Tregs in para-aortic LNs (n=8-13 **(i)**) and spleen (n=8-13 **(j)**). **(a-j)** Data represent mean±SEM. **P*<0.05; ***P*<0.01; ****P*<0.001 versus control, TGFβ or *Apoe*^{-/-}*Ccl17*^{wt/e} mice, as analyzed by Student's t-test with Welch correction or Kruskal-Wallis with Dunn's multiple comparisons test, as appropriate.

Figure 8. CCL3 drives atherosclerosis and mediates reduced Treg numbers *in vivo*

(a, b) Flow cytometric quantification of CD45⁺CD3⁺CD4⁺CD25⁺FoxP3⁺ Tregs in the para-aortic LNs (n=10) **(a)** and spleens (n=6-10) **(b)** of *C57Bl/6* or *Ccl3*^{-/-} mice. **(c)** Experimental scheme of *Apoe*^{-/-} or *Apoe*^{-/-}*Ccl3*^{-/-} mice fed a WD for 12 weeks. **(d)** Representative images and quantification of lesion area measured after Oil-Red-O staining for lipid deposits in the aortic root of *Apoe*^{-/-} or *Apoe*^{-/-}*Ccl3*^{-/-} mice (n=13-18). Scale bar = 500 μm. **(e)** Quantification of lesion area measured after Oil-Red-O staining for lipid deposits in the thoraco-abdominal aorta of *Apoe*^{-/-} or *Apoe*^{-/-}*Ccl3*^{-/-} mice (n=13-16); **(f)** Representative images and atherosclerotic lesion size of aortic arches quantified in *Apoe*^{-/-} or *Apoe*^{-/-}*Ccl3*^{-/-} mice (n=8-14) using H&E staining. **(g, h)** Flow cytometric quantification of CD45⁺CD3⁺CD4⁺CD25⁺FoxP3⁺ Tregs in para-aortic LNs (n=13-17) **(g)** and spleen (n=13-18) **(h)** of *Apoe*^{-/-} or *Apoe*^{-/-}*Ccl3*^{-/-} mice. **(i)** Experimental scheme of *Apoe*^{-/-} or *Apoe*^{-/-}*Ccl17*^{oe/e} mice fed a WD for 4 weeks and injected 3x weekly with or without recombinant mouse CCL3 (20 μg i.p.). **(j)** Representative images and quantification of lesion area measured after Oil-Red-O staining for lipid deposits in the aortic root of *Apoe*^{-/-} or *Apoe*^{-/-}*Ccl17*^{oe/e} treated with PBS or CCL3 (n=6-8). Scale bar = 500 μm; **(k,l)** Flow cytometric quantification of CD45⁺CD3⁺CD4⁺CD25⁺FoxP3⁺ Tregs in para-aortic LNs (n=7-9) **(k)** and spleen (n=7-9) **(l)**. **(a-l)** Data represent mean±SEM. **P*<0.05, ***P*<0.01; ****P*<0.001 versus *Apoe*^{-/-}, as analyzed by Student's t-test with Welch correction, Mann-Whitney test, or Kruskal-Wallis with Dunn's multiple comparisons test, as appropriate.

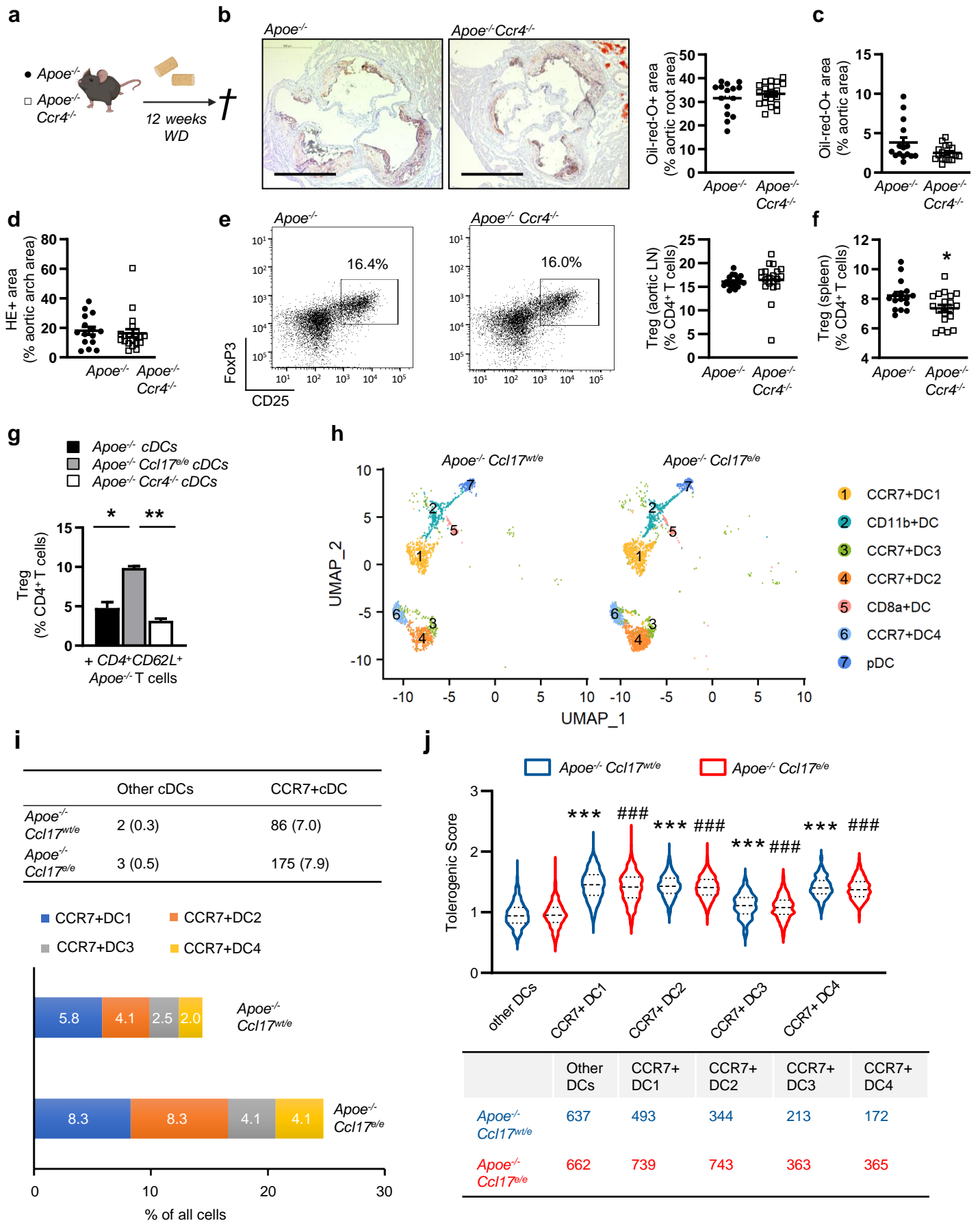


Figure 1

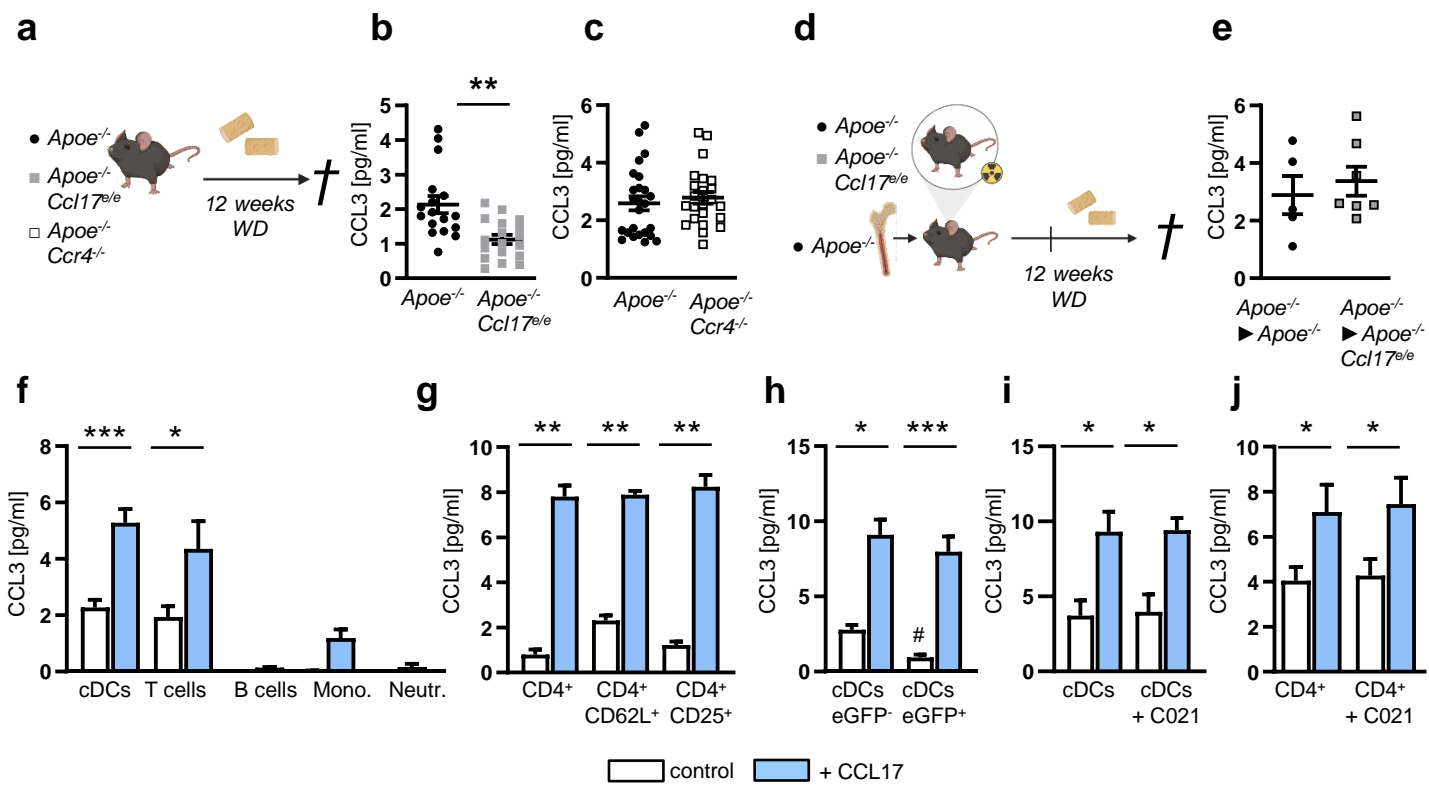


Figure 2

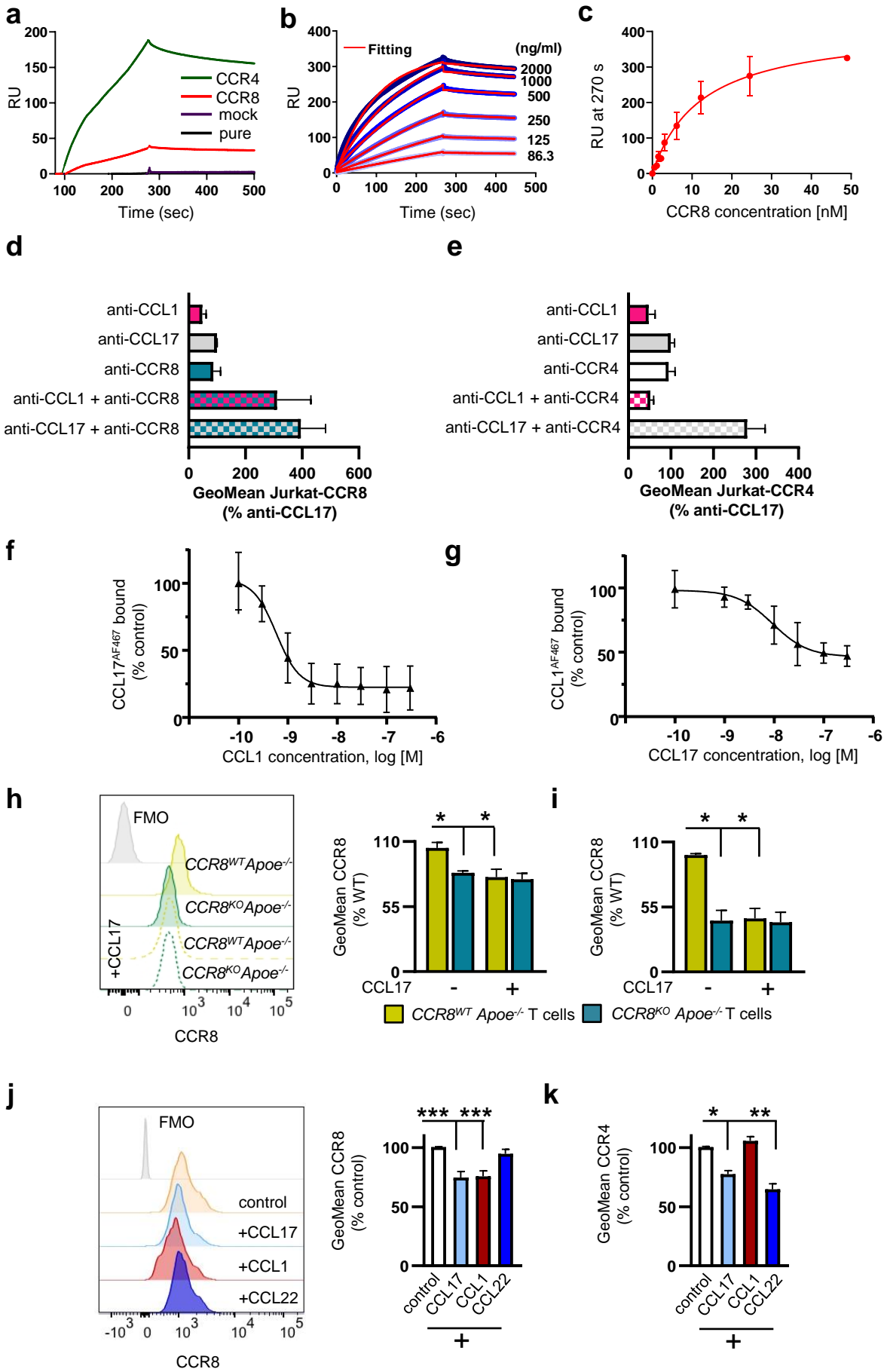


Figure 3

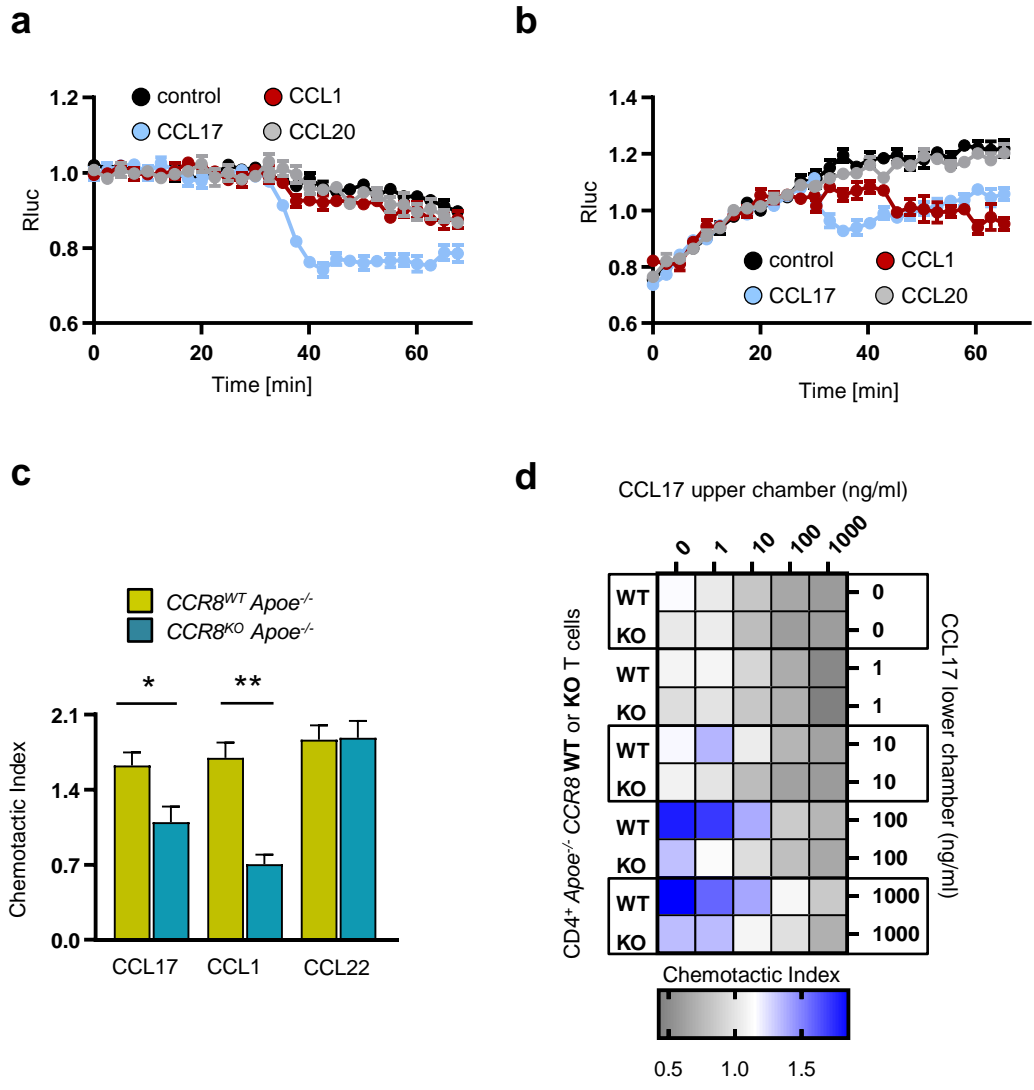


Figure 4

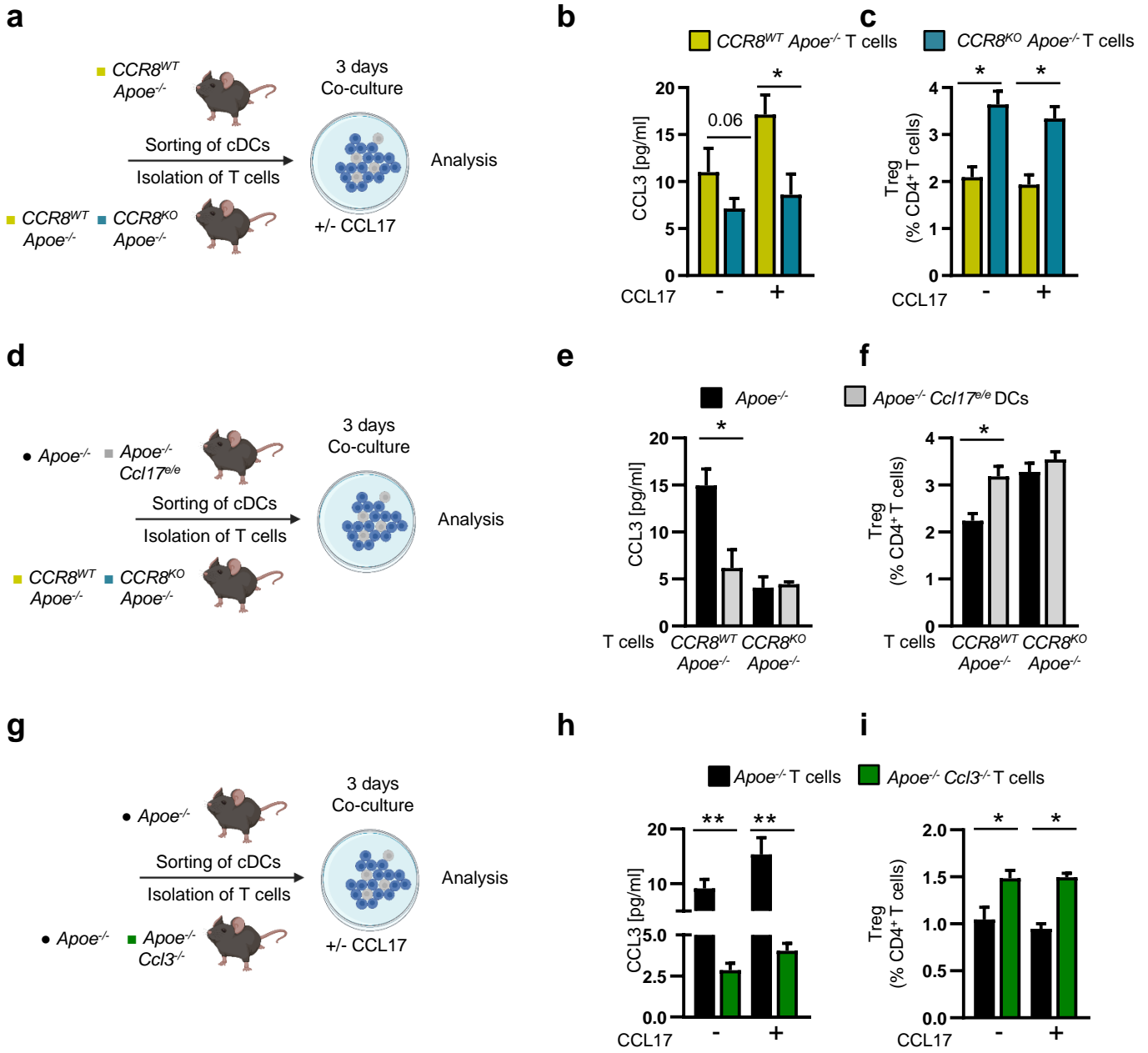


Figure 5

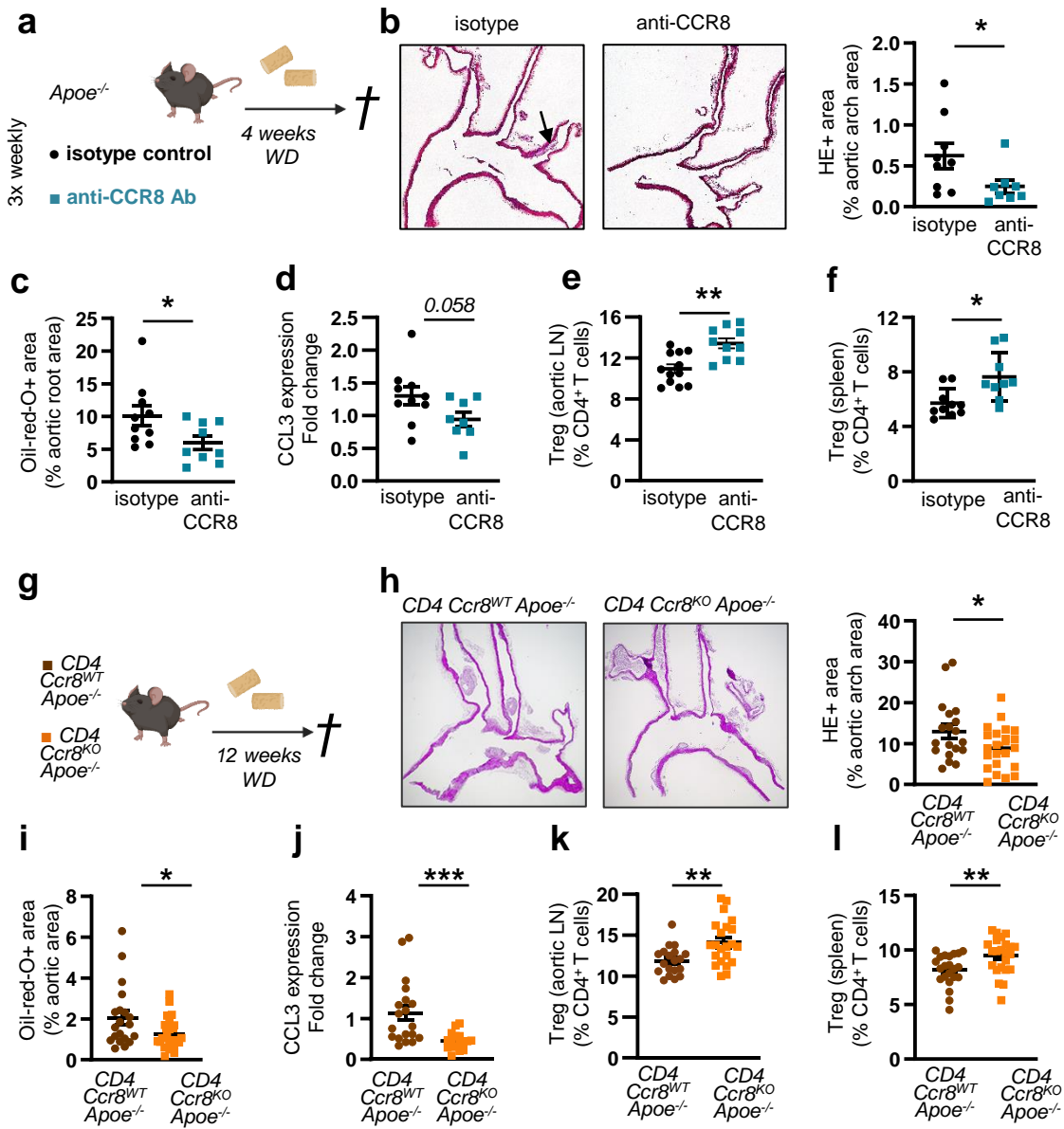


Figure 6

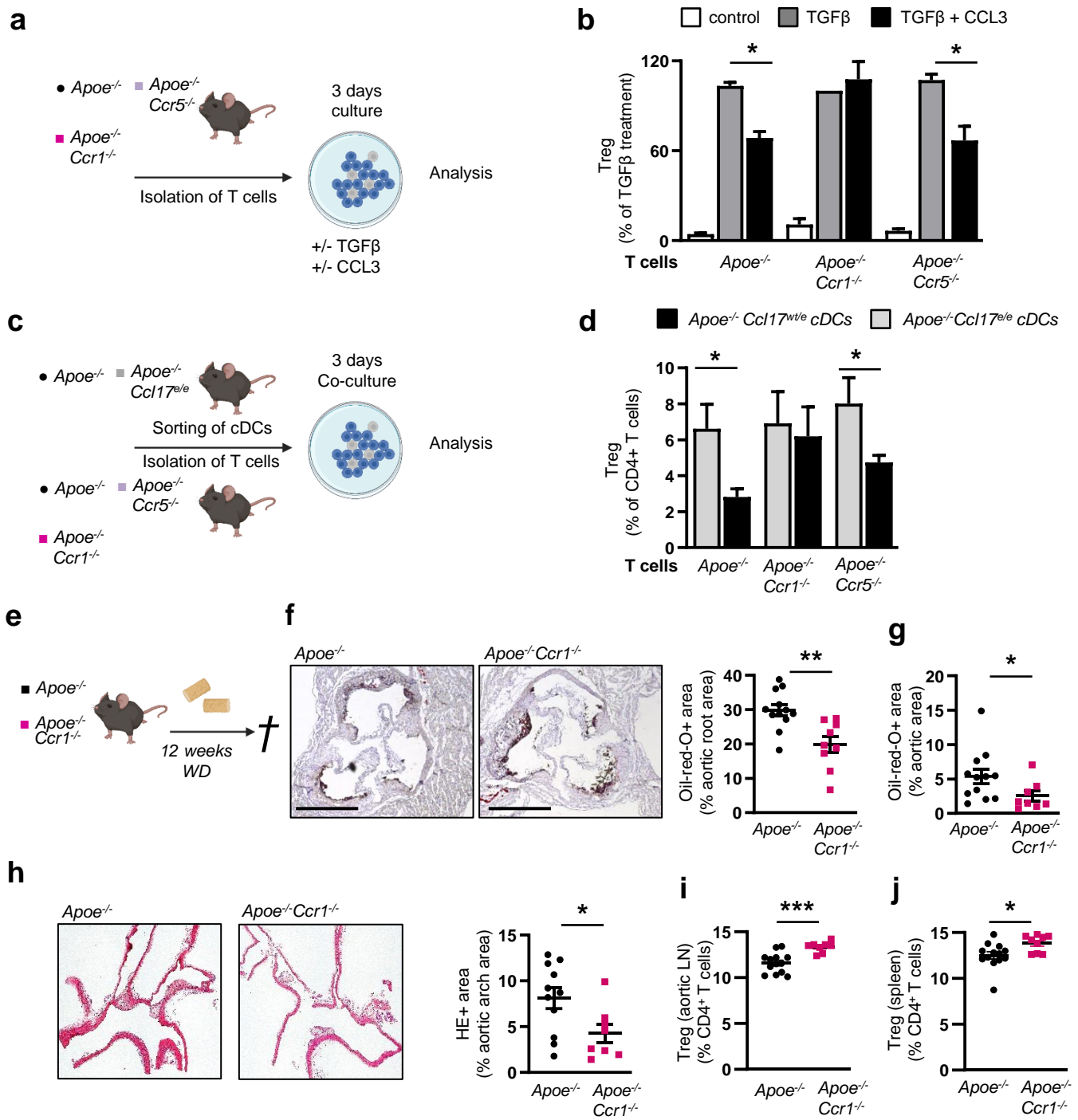


Figure 7

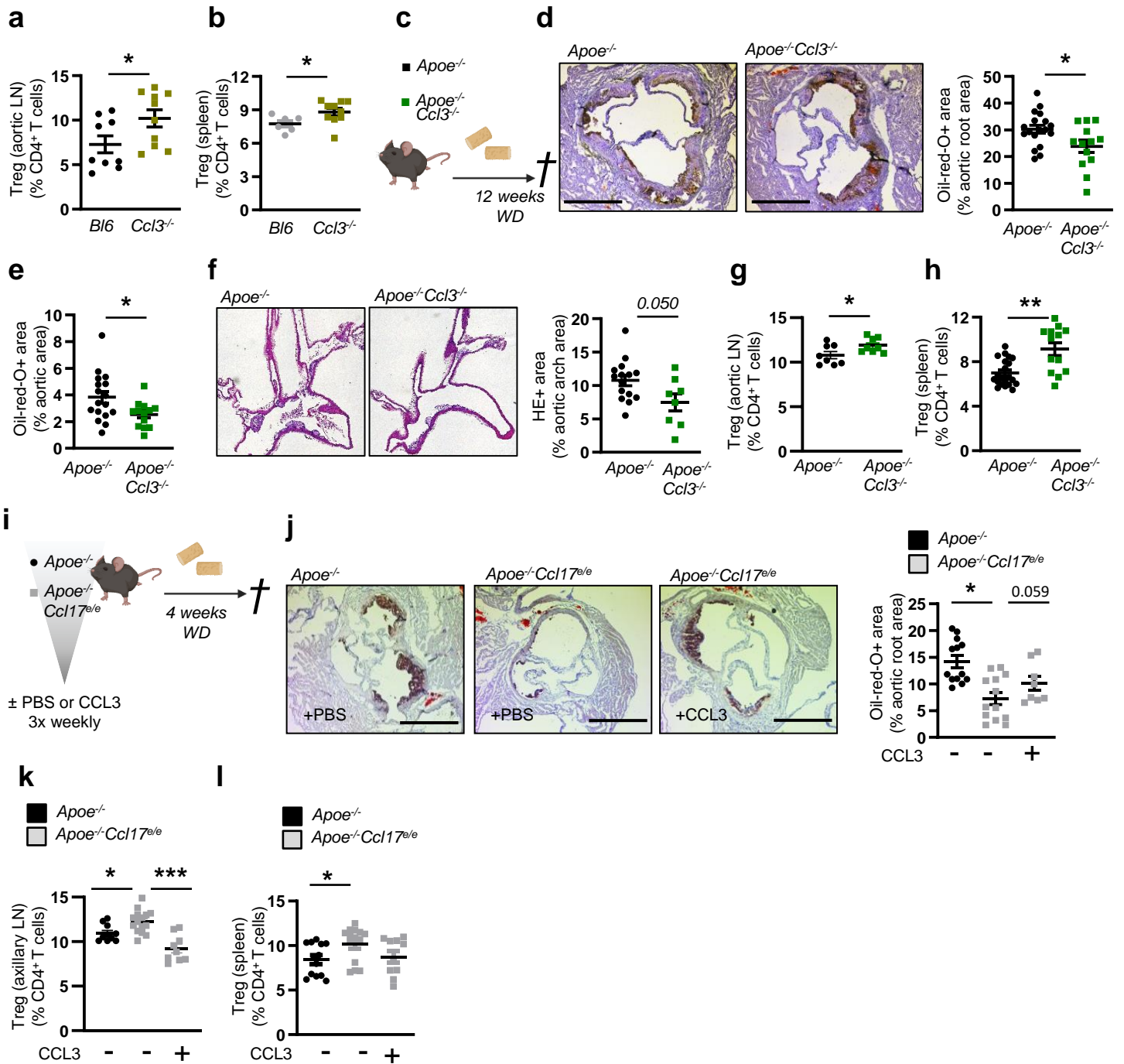


Figure 8